European Journal of Medicinal Chemistry 238 (2022) 114514

Contents lists available at ScienceDirect

European Journal of Medicinal Chemistry

journal homepage: www.elsevier.com/locate/ejmech

Design and synthesis of a novel non peptide CN-NFATc signaling inhibitor for tumor suppression in triple negative breast cancer

Adrià Sánchez-Morales [a,3], Atilla Biçer [b,1,3], Vasilis Panagiotopoulos [c,3], Selma Crecente-Garcia [a,2], Cristina Benaiges [a], Sergi Bayod [d], José Luís Hernández [d], Félix Busqué [a], Minos-Timotheos Matsoukas [c,***], Mercè Pérez-Riba [b,**], Ramon Alibés [a,*]

[a] Departament de Química, Universitat Autònoma de Barcelona, Bellaterra, Barcelona, 08193, Spain
[b] Genes, Disease and Therapy Program, Human Molecular Genetics Laboratory, Bellvitge Biomedical Research Institute (IDIBELL), L'Hospitalet de Llobregat, Barcelona, 08908, Spain
[c] Department of Biomedical Engineering, University of West Attica, Egaleo, Athens, 12210, Greece
[d] Health & Biomedicine Department of LEITAT Technological Center, Parc Científic de Barcelona, Hèlix building. Baldiri Reixach 15-21, Barcelona, 08028, Spain

ARTICLE INFO

Keywords:
Docking-based design
Druggability evaluation
SAR exploration
Calcineurin
NFAT signaling Inhibitor
Triple negative breast cancer
PxIxIT

ABSTRACT

The $Ca2^{+}$/calmodulin-mediated phosphatase activity of calcineurin (CN) integrates calcium-mediated signaling with gene expression programs involved in the control of essential cellular processes in health and disease, such as the immune response and the pathogenesis of cancer progression and metastasis. In addition, CN is the target of the immunosuppressive drugs cyclosporine A (CsA) and FK-506 which are the cornerstone of immunosuppressant therapy. Unfortunately, long-term administration of these drugs results in severe side effects. Herein, we describe the design, synthesis and evaluation of new synthetic compounds that are capable of inhibiting NFATc activity in a dose-dependent manner, without interfering on CN phosphatase activity. These compounds were designed using the structure-based pharmacophore model of a peptide-derived PxIxIT sequence binding to calcineurin A subunit. Moreover, these compounds inhibit NFATc-dependent cytokine gene expression, secretion and proliferation of human T $CD4^{+}$ cells. More importantly, compound **5a** reduces tumor weight and shows a tendency to reduce tumor angiogenesis in an orthotopic immunocompetent mouse model of triple negative breast cancer, suggesting that **5a** has tumor suppressor activity. These findings validate compound **5a** as an agent with therapeutic activity against CN-NFATc and highlight its potential as a tool for drug development with therapeutic purposes.

1. Introduction

Calcineurin (CN) or protein phosphatase 3 (PPP3, formerly PP2B) is highly conserved in eukaryotic cells and ubiquitously expressed, and the only Ca^{2+}-calmodulin-regulated serine/threonine protein phosphatase [1,2]. CN functions as a heterodimer that consists of a calmodulin-binding catalytic subunit A, CNA, and a Ca^{2+} binding regulatory subunit B, CNB. Intracellular increase of Ca^{2+} activates CN which dephosphorylates fourteen residues of the transcription factor family Nuclear Factor of Activated T-cells 1 to 4 (NFATc1 to NFATc4, hereafter referred as NFATc) inducing nuclear translocation, where they bind to DNA and activate the transcription of many genes. Therefore, CN-NFATc signaling integrates calcium signaling with gene expression programs to allow control of essential cellular processes in health and disease such as the immune response and the pathogenesis of cancer and metastasis [3–7].

Two short linear motifs (SLiMs) of NFATcs, the PxIxIT and the πΦLxVP (where π corresponds to polar and Φ to hydrophobic amino acid residues; hereafter referred as LxVP), are involved in CN binding and cell

* Corresponding author.
** Corresponding author.
*** Corresponding author.
E-mail addresses: mmatsoukas@uniwa.gr (M.-T. Matsoukas), mpr@idibell.cat (M. Pérez-Riba), ramon.alibes@uab.cat (R. Alibés).
[1] Presently working at Centre for Genomic Regulation (CRG), Systems Biology Programme. Aiguader 88, Barcelona, 08003, Spain.
[2] Present address: School of Chemistry, University of Bristol, Cantock's Close, Bristol BS8 1TS, United Kingdom.
[3] These authors contributed equally.

https://doi.org/10.1016/j.ejmech.2022.114514
Received 11 April 2022; Received in revised form 1 June 2022; Accepted 2 June 2022
Available online 4 June 2022

Abbreviations

CN	Calcineurin
CNA	Catalytic subunit A of CN
DIPEA	*N*,*N*-Diisopropylethylamine;
EDCI	1-Ethyl-3-(3-dimethylaminopropyl)carbodiimide;
HATU	Hexafluorophosphate Azabenzotriazole Tetramethyl Uronium
HOBt	Hydroxybenzotriazole
hPMBC	Human peripheral blood mononucleated cells
IHC	Immunohistochemistry
NFATc	cytosolic Nuclear Factor of Activated T Cells
SLiM	Short Linear motifs
TNBC	Triple Negative Breast Cancer

signaling [8,9]. Protein chemistry and X-ray crystallography established that the NFATc PxIxIT sequence, which is the main anchoring sequence to CNA, aligns along the β-strand 14 extending the CNAβ sheet where it is located [10,11]. As to the NFATc LxVP motif, it binds at the CNA/CNB interface, and it has been suggested to be involved in proper positioning of NFATc phosphosites to the active site of CNA [8,12].

CN recognizes and binds regulators, substrates or scaffolding proteins that include both PxIxIT and/or LxVP motifs [6–8,13,14]. Protein-derived SLiMs motifs from modulators of CN compete with the SLiMs peptide sequences on NFATcs for binding to CN and by these means they interfere with NFATc cell signaling [6]. Structural analysis of protein modulators, substrates and scaffold proteins binding to CN showed that both short degenerate PxIxIT and LxVP SLiMs bind in intrinsically disordered proteins/regions at the corresponding PxIxIT- and LxVP- binding pockets in CN. Interestingly, the same NFATc PxIxIT binding structure of adding a ß strand to the edge of a ß sheet of CNA was described in several CN modulators such as for the PKIIIT from the African swine fever virus protein A238L [12], the IAIIIT from the A-kinase anchoring protein 5 of 79 kD (AKAP79) protein [15], and the PSVVVH from RCAN1 protein [16]. Remarkably, these protein-derived PxIxIT peptides when bound to CN do not affect either substrate binding to CN or overall CN phosphatase activity [17,18], which highlights the therapeutic importance of these peptides and of the CN PxIxIT binding –site pocket as a target to regulate CN-NFATc signaling in disease.

The relevance of NFATcs cell signaling is also highlighted by the fact that the immunosuppressant drugs cyclosporine A (CsA) and FK506 (tacrolimus), in complex with intracellular immunophilins, bind to CN at the same CN-binding LxVP pocket, blocking access and binding to the CN active site for all substrates, and sterically hindering the phosphatase activity of CN [12,19–22]. Both drugs are nowadays the cornerstone of the immunosuppressant therapy. Unfortunately, long-term administration of these drugs provokes severe side effects such as neurotoxicity, renal dysfunction, hypertension and diabetes [23,24]. Therefore, there is an unmet medical need to identify new immunosuppressant molecules, alternative to CsA and FK506, which selectively inhibit CN-NFATc signaling without affecting the phosphatase activity of CN towards substrates. If these molecules mimicked the PxIxIT and/or the LxVP SLiMs function, they could be valuable novel selective pharmacological tools to avoid pathological aberrations resulting from the imbalance in the CN-NFATc pathway in pathological conditions.

The therapeutic potential of the protein derived PxIxIT peptides is affected by their low bioavailability and/or limited stability that compromises their utility in clinical therapy. In this context, taking advantage of the crystal structure of CN in complex with the AKAP79-derived peptide EPIAIIITDTE including the PxIxIT sequence IAIIIT [15], we previously developed a structure-based pharmacophore model with the aim of identifying small non-peptidic compounds that inhibit CN-NFATc signaling, which could act as drug candidates for immunosuppressive therapy [25]. From the potential candidates identified, it was found that four small non-peptide hit molecules (Fig. 1) strongly inhibit NFATc-dependent gene expression, cytokine production and proliferation of activated human $CD4^+$ T lymphocytes, uncovering their therapeutic potential as immunosuppressive agents [25].

Herein, using the computationally calculated binding characteristics of the discovered compounds to CNA, we have designed and synthesized two new compounds, **5a** and **5e**, that are capable of inhibiting NFATc-dependent cytokine secretion and proliferation of human $CD4^+$ T cells. We demonstrate that they have potential immunosuppressant activity and modulate *in vitro* and *in vivo* CN-NFATc signaling (*vide supra*). In addition, compound **5a** reduces tumor growth and shows a tendency to reduce tumor angiogenesis in an orthotopic syngeneic mouse model of triple negative breast cancer, corroborating its tumor-suppressor activity.

2. Results

The computationally calculated binding characteristics of the compounds to CN found in our previous study [25] show that a common feature of these compounds is the sulfone-aromatic-carbonyl groups which mimic the interactions of PxIxIT peptides with the β-sheet of CNA, in an area which can be compartmentalized in three parts, hydrophobic 1 (HYD1), hydrophobic 2 (HYD2) and polar (POL) (Fig. 2A-B). In particular, the two sulfone oxygens interact with CNA by forming two hydrogen bonds with the N330 side chain and Q333 main chain NH hydrogens (Fig. 2A-B, HYD1 and HYD2) in an area of the binding site characterized by polar interactions (Fig. 2A-B, POL). Furthermore, HYD1 can be attributed to the hydrophobic interactions between ligand and I331 and Y288, and HYD2 to the remainder of the greater hydrophobic pocket, formed by M329, F299, P300 and M290. The common carbonyl group of compounds **1–4** was proposed to interact with the main chain NH of I331 in HYD1.

The strategy to design new CN-NFATc inhibitors was either to eliminate functional groups not relevant to the initial proposed interaction patterns, or to switch functional groups to produce higher affinity compounds without losing any of the important interactions of the hit compounds. Considering the interactions of compound **3** (Fig. 2A), the set of compounds **5a-e** was designed on the basis of first modifying the 2-methylindoline group scaffold by removing 3 carbon atoms from the methylpyrrolidine, thus, switching to an aniline moiety. This would simplify the molecule scaffold while retaining the crucial interactions, namely aromaticity in HYD1 and the carbonyl hydrogen bond with the main chain NH of I331. Second, eliminating the isopropyl benzene, which has no apparent interactions and is facing towards the solvent, and third, replacing the methoxybenzene with 5 different cyclic or bicyclic aromatic or heteroaromatic groups (**a-e**), to retain the aromaticity but adding additional hydrogen bond donors or acceptors. In the case of compound **4** (Fig. 2B), a similar design strategy was employed to design the set of compounds **6a-f**. In particular, the scaffold remained the same benzyl and sulfone group. The chlorobenzene group and the attached sulfonamide amine were removed due to the lack of any apparent interactions with CNA, and the 2,5-dimethylthiophene was replaced by cyclic or bicyclic aromatic or heteroaromatic groups (**a-f**). Therefore, two small libraries of carboxamides **5a-e** (from compound **3**) and **6a-f** (from compound **4**) were designed as potential CN-NFATc signaling inhibitors (Fig. 2C). The novel compounds bear a sulfonamide or a sulfone group at either end of the molecule and an aromatic moiety: indole, naphthalene, thiophene, ethylbenzene or benzothiophene. Compounds **5a-e** consisted of a methane sulfonamide linked *via* a methylphenyl tether to the different aromatic and heteroaromatic amides, while compounds **6a-f** consisted of a methyl sulfonyl group linked *via* an *N*-phenylamino 2-oxoethyl tether to the different aromatic and heteroaromatic amides.

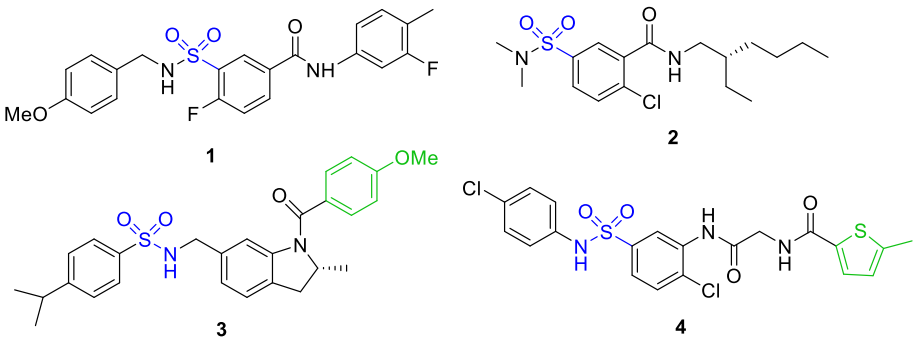

Fig. 1. Hit CN-NFATc signaling inhibitors found by virtual screening: **1**, ZINC20664716; **2**, ZINC7608489; **3**, ZINC65003396 and **4**, ZINC13038446 [25].

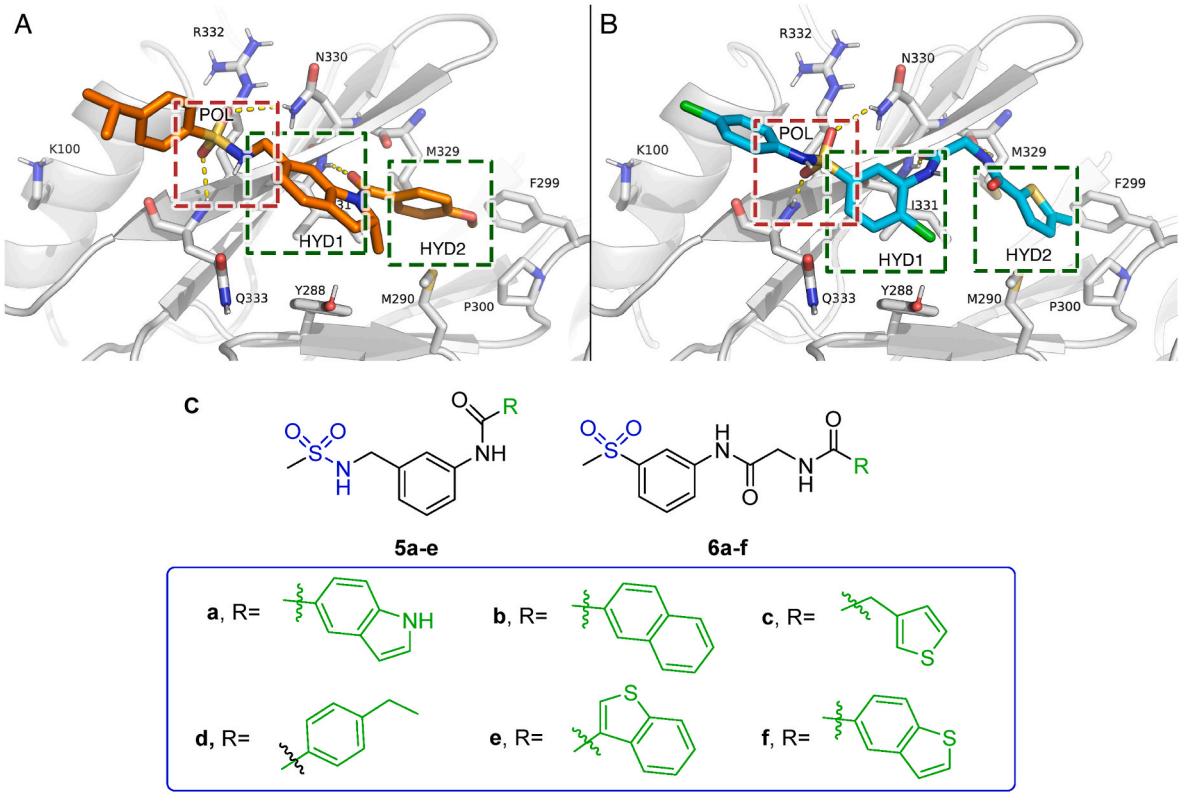

Fig. 2. A: Compound **3** (ZINC65003396) depicted in orange color, docked into the PxIxIT binding pocket of CNA (grey) and breakdown of the interaction subpockets. POL, HYD1 and HYD 2 correspond to the three defined areas of CNA, interacting with distinct functional groups of the compound. **B:** Compound **4** (ZINC13038446) in cyan color, docked into the PxIxIT binding pocket of CNA and corresponding subpockets. **C:** Proposed families **5a-e** and **6a-f** of new CN-NFATc inhibitors.

2.1. Chemistry

The new set of carboxamides **5a-e** was prepared by a linear sequence according to Scheme 1 starting from commercially available 3-nitrobenzylamine **7**. Thus, the synthesis of the pivotal intermediate **9** was achieved in almost quantitative yield by the reaction of mesyl chloride with amine **7** [26] followed by the reduction of the nitro group on sulfonamide **8**. Then, amine **9** was tethered to commercially available aromatic and heteroaromatic carboxylic acids **10a-e** using the carbodiimide coupling reagent EDCl·HCl along with HOBt and DIPEA as base [27] to afford the corresponding carboxamides **5a-e.**

The synthesis of carboxamides **6a-f** began with commercially available 3-mehylsulfonyl aniline **11** following the strategy outlined in Scheme 2. Accordingly, *N*-Boc protected glycine **12** was tethered to compound **11** using HATU as the coupling reagent [28] and DIPEA in THF leading to derivative **13** in 51% yield. Initial attempts to carry out the coupling reaction using the EDCl/HOBt system gave lower yields. Removal of the *tert*-butyl carbamate protection of **13** by treatment with TFA in DCM [29] furnished common intermediate **14**, onto which the aromatic and heteroaromatic carboxylic acids **10a-f** were introduced. This was performed using EDCl·HCl promoted amide formation under standard conditions to deliver the target carboxamides **6a-f.**

2.2. Newly synthesized non-peptide small molecules partially disrupt CNA-NFATc derived PRIEIT peptide interaction

The synthesized compounds **5a-e** and **6a-f** were submitted to competitive binding studies to CNA with carboxyfluorescein (CF) labelled NFATc2-derived PRIEIT peptide (CF-PRIEIT), using fluorescence polarization (FP) assays at 10 μM and 100 μM peptide concentration (Fig. 3A). The human NFATc2 derived CF-PRIEIT (amino acids 108–119) and the RCAN3 derived CF-R3 (amino acids 191–202

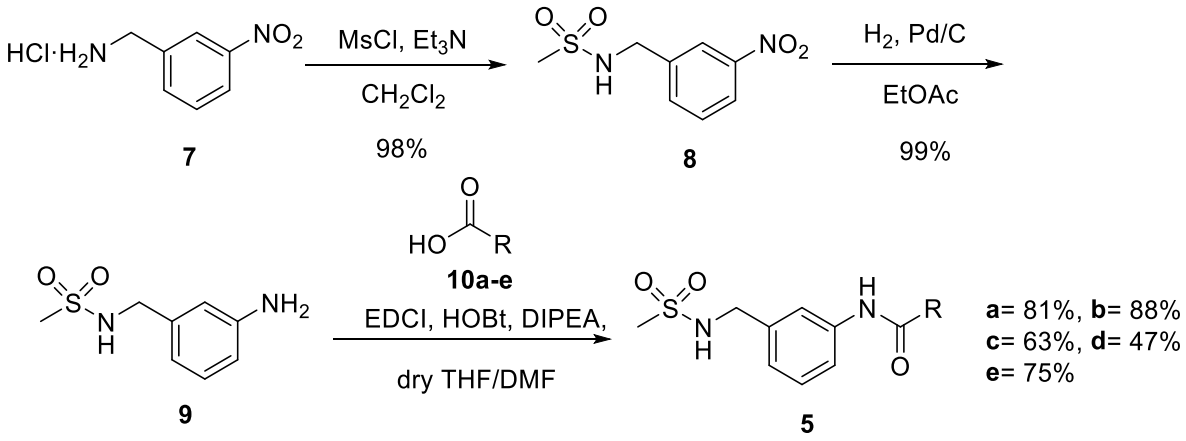

Scheme 1. Synthesis of carboxamides **5a-e**.

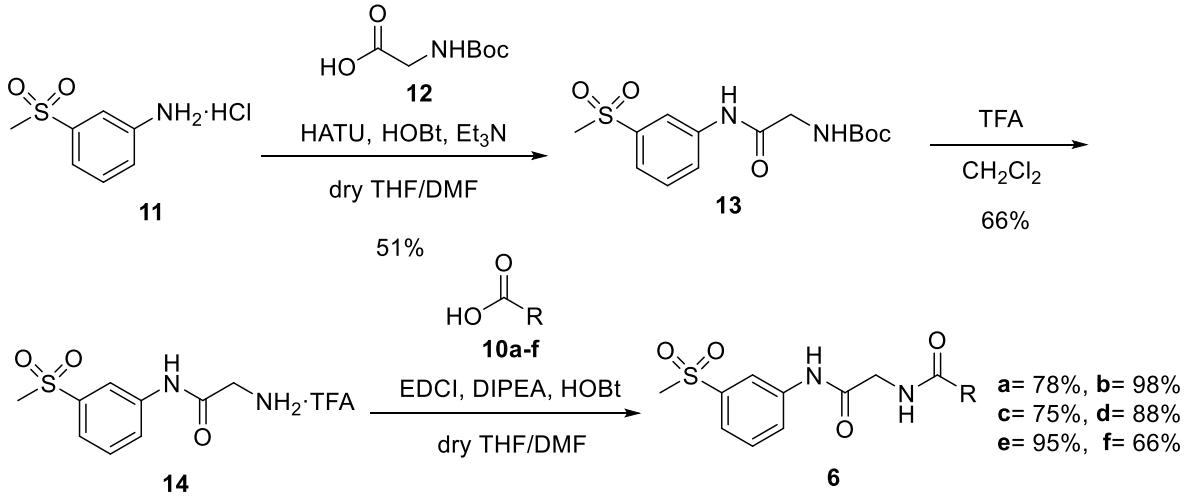

Scheme 2. Synthesis of carboxamides **6a-f**.

including the PxIxIT sequence PSVVVH) peptides were used as positive controls for the disruption of the CNA – CF-PRIEIT interaction. The R3 peptide with three-point mutations at the PxIxIT motif, the PSVAAQ (CF-R3 mut) peptide, and compound **15** (Fig. 3B) were used as negative controls of PRIEIT displacement from CNA**.** The disruption of the interaction between CNA and the CF-NFATc2-derived PRIEIT (CF-PRIEIT) peptide induced by the compounds was analyzed by FP analysis. Compounds **5a**, **5c**, **5d** and **5e** at 100 μM, but not **5b** and family **6** compounds, partially disrupt the CNA – CF-PRIEIT interaction (Fig. 3A) to a similar degree as the previously described compound **4** [25], a potent inhibitor of NFATc activity. However, at 10 μM, only compounds **5a** and **5c** partially displace the CF-PRIEIT interaction with CNA to different extents.

In order to examine the interaction mechanism of these compounds, they were docked in the CNA - PxIxIT interaction interface. In accordance with the predicted binding model of compound **4**, compound **5a** demonstrated the same pattern, in which the sulfonamide oxygen and NH atoms form hydrogen bonds with the side chain NH of N330 and the carbonyl of Q333 respectively (Fig. 3C, yellow). Hydrogen bonds are also formed between the amide and indole NH atoms and M329 and N327 main chain carbonyl oxygens, respectively. As expected, the HYD1 and HYD2 (Fig. 2A–B) subpockets are occupied by the phenyl and indole groups. The phenyl group forms hydrophobic interactions with I331, M290 and Y288 side chains in the HYD1 subpocket, while the indole group is placed in HYD2 interacting with F299 and M329, stabilized by an extra hydrogen bond with N327. Accordingly, for compound **5e**, the sulfonamide oxygen and NH atoms form hydrogen bonds with the main chain NH of I331 and carbonyl of Q333, respectively, consistent with the notion that the sulphone group in the series interacts with either N330 or Q333 through hydrogen bonding (Fig. 3D, blue). A hydrogen bond is also formed between the amide group and the M329 main chain carbonyl oxygen. As expected, HYD1 and HYD2 subpockets are occupied by the phenyl and benzothiophene group. What is observed in the case of **5a**, in contrast to the other compounds in the series, is the extra hydrogen bond formed by the indole group NH to N327, which may provide the basis for understanding its increased displacement capability towards the CNA - PxIxIT binding pocket.

2.3. Most compounds of family 5, but not compounds from family 6, inhibit NFATc dependent transcriptional activity without blocking phosphatase activity of CNA

Potential immunosuppressant CN-NFATc signaling inhibitors should compete with NFATc for binding to CN without blocking its phosphatase activity. In this context, the phosphatase activity of CNA was assessed using the small molecule *p*-nitrophenyl phosphate (pNPP) as substrate. Neither compounds **5a-e** nor **6a-f** affect CNA phosphatase activity towards pNPP (Fig. 4A left and right panel, respectively). In contrast, $ZnCl_2$, which was used as a positive control of inhibition of CNA phosphatase activity, markedly inhibits the enzyme phosphatase activity.

The ability of the family of compounds **5** and **6** to directly inhibit NFATc transcriptional activity was evaluated in human HEK 293T cells

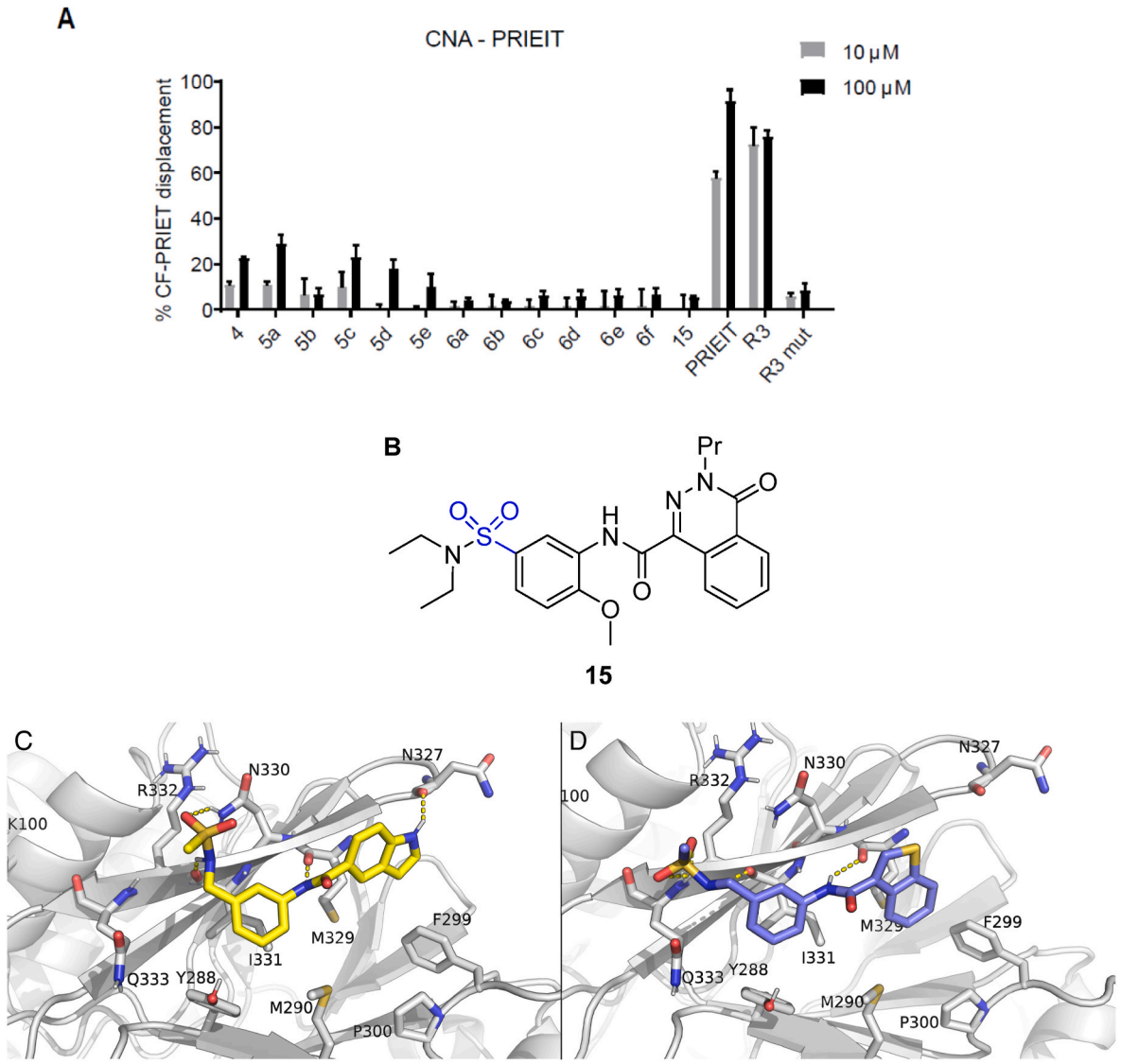

Fig. 3. Newly synthesized non-peptide small molecules partially disrupt CNA-NFATc derived PRIEIT peptide interaction. **A:** Fluorescence polarization analysis of the disruption of the CNA – CF-NFATc2-derived PRIEIT (CF-PRIEIT) peptide interaction induced by the compounds under study. The fluorescence polarization of the free CF-PRIEIT peptide was considered 100% of displacement and the binding of CNA to the CF-PRIEIT peptide in absence of any compound was considered 0% displacement. The human NFATc2 (UniProtKB ID: Q13469-1) derived CF-PRIEIT (amino acids 108–119) and the RCAN3 (UniProtKB ID: Q9UKA8-1) derived CF-R3 (amino acids 191–202 including the PxIxIT sequence PSVVVH) peptides were used as positive controls for the disruption of the CNA – CF-PRIEIT interaction. The R3 peptide with three-point mutations at the PxIxIT motif, the PSVAAQ (CF-R3 mut) peptide and compound **15** were used as negative controls of PRIEIT displacement from CNA. Compound displacement percentage at 10 μM and 100 μM of CF-PRIEIT peptide (5 nM) from CNA interaction (12 μM). **B:** Compound **15** was used as a negative control of CNA-NFATc disruption. **C:** Docked pose of **5a** (yellow) in the CNA - PIxIxT binding pocket (grey). **D:** Docked pose of **5e** (blue) to CNA (grey). Hydrogen bonds are highlighted in yellow dashed lines.

using a luciferase gene reporter assay of the NFATc-dependent *IL2* promoter (3xNFATc-luc), the promoter activity of which is regulated by NFATc. As a control of internal transfection efficiency, the plasmid pRLnull was used, with a promoter not regulated by NFATc. Compound **15** was used as a negative control of inhibition of the NFATc transcription activity. As no previous data on cell permeability or stability of these compounds was available, the cells were incubated with each compound for 2 h prior to cell stimulation with ionomycin (Io) and phorbol 12-myristate 13-acetate (P), Io + P stimulation for 4 h, to determine their effect on NFATc activity. As control for NFATc activity inhibition, cells were treated with CsA for 30 min before Io + P stimulation. Compounds **5a**, **5e** as well as **4** inhibit more than 80% NFATc activity, while compounds **5c** and **5d** inhibit 60–75% NFATc activity at 50 μM compound concentration (Fig. 4B, left panel). Compounds **5b** and **6a-f** (Fig. 4B, left and right panel), as the negative control compound **15**, barely inhibit NFATc activity at the given concentrations under the experimental conditions used. In conclusion, compounds **5a**, **5c**, **5d** and **5e**, like compound **4**, partially displace CF-PRIEIT binding to CNA but strongly inhibit NFATc activity at 50 μM, without affecting the general phosphatase activity of CN. Next, considering that compounds **5a** and **5e** presented the highest NFATc inhibitory activity without affecting CNA phosphatase activity, we decided to focus on both compounds to explore their capability to inhibit NFATc activity in a dose-response manner. Dose-response assays of NFATc-dependent luciferase reporter gene expression were carried out as before but treating cells with increasing concentrations of **5a**, **5e** and **4** for 2 h prior to cell stimulation, followed by stimulation with Io + P for 4 h. All compounds except CsA and compound **15**, used as negative controls of NFATc activation, inhibit NFATc activity in a dose-dependent manner for concentrations ranging from 0.1 μM to 50 μM (Fig. 4C). Analysis of the dose response data in a

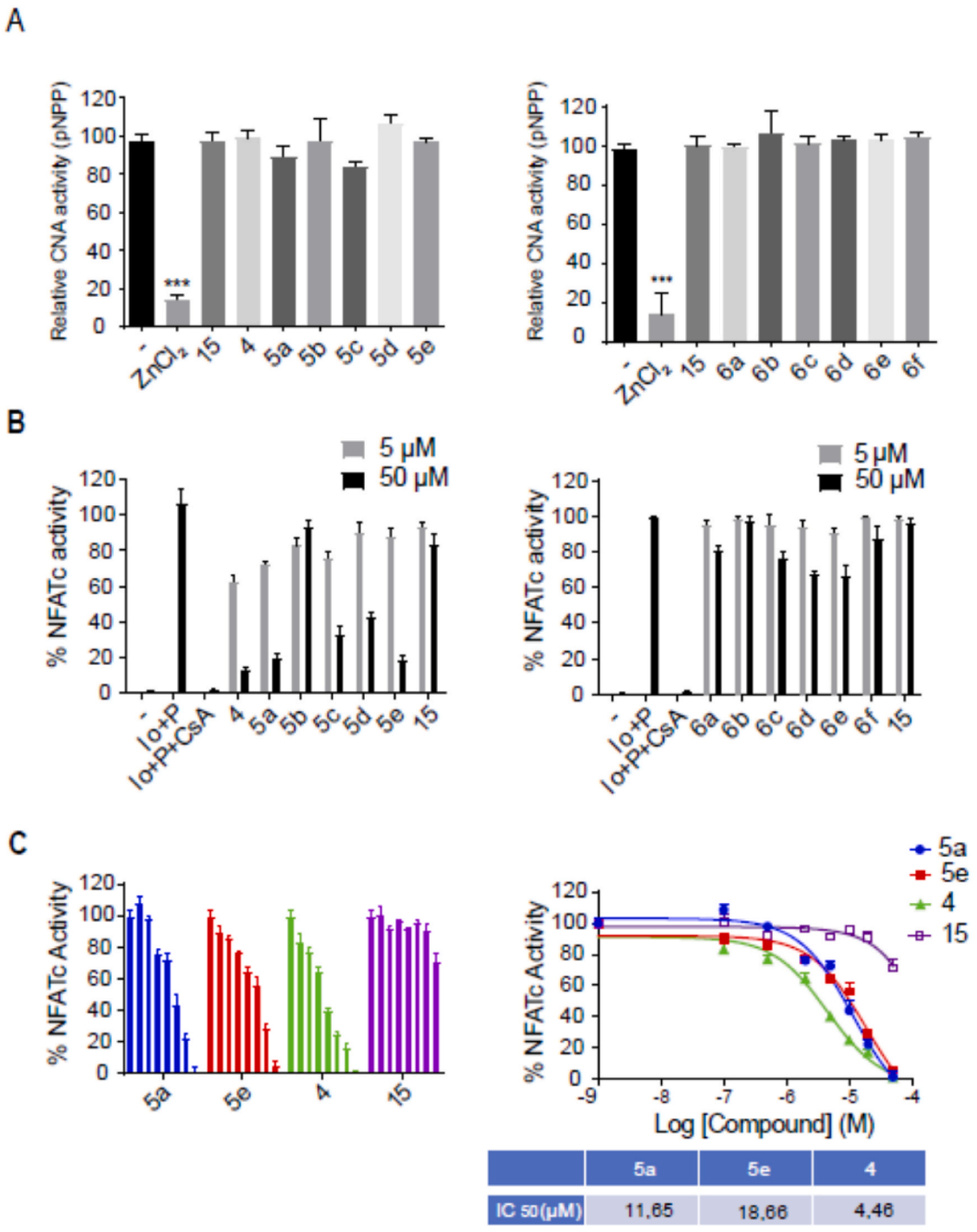

Fig. 4. Compounds **5a** and **5e** have the highest NFATc inhibitory activity without affecting CN phosphatase activity. **A:** Human recombinant CNA phosphatase activity towards the pNPP substrate in the presence of families **5** (left) and **6** (right). Results are shown as percentage of CNA phosphatase activity in the presence of 50 µM of each compound relative to the CNA activity in the absence of any compound (100% value). As a positive control for CNA phosphatase activity inhibition, 1 µM $ZnCl_2$ was added. CNA activity in the absence of compounds is shown as a black dash (positive control of CN activity). Data is given as mean ± SD of 3 independent experiments with triplicates. Statistical significance was determined with 2-way ANOVA test (***$p < 0.001$, *$p < 0.05$). **B:** NFATc activity in human HEK 293T cells. The activity was analyzed using the 3xNFAT-luc reporter gene after 2 h of cell treatment with each compound (50 µM and 5 µM) prior and during cell stimulation with 1 µM ionomycin (Io), 2 mM $CaCl_2$, and 20 ng/ml phorbol 12-myristate 13-acetate (P) (Io + P) for 4 h. NFATc activation achieved upon cell stimulation with Io + P for 4 h in the absence of any compound corresponds to the 100% value. As control for NFATc activity inhibition, cells were treated with 1 µM cyclosporin A (CsA) for 30 min before Io + P stimulation. Compound **15** was used as a negative control of inhibition of NFAT transcriptional activity. Luciferase activity was measured from crude protein extracts. Data is given as mean ± SD of 3 independent experiments with triplicates. **C: On left,** Dose-response assays of NFAT activity with 3xNFAT-luc reporter gene were performed in HEK 293T cells. Cells were treated with each compound at 0/0.1/0.5/2/5/10/20/50 µM (increasing concentrations of the compounds are represented in the graph from left to right) for 2 h and then were calcium stimulated with Io + P for 4 h as described in B. Values are given as percentage of NFATc activation in the presence of each compound relative to the 100% NFATc activity value of the positive control. Data corresponds to the mean ± SD of 3 independent experiments with triplicates. **On right,** data is represented as a dose response curve plotted in a XY dispersion graph. IC_{50} values were calculated using a non-linear regression curve (three-way) with GraphPad Prism8.

XY dispersion graph indicates that these compounds bind to CNA and are strong inhibitors of NFATc activity in the low micromolar range (IC_{50} values for **5a**, **5e** and **4** were 11.6, 18.7 and 4.5 μM, respectively; Fig. 4C right panel).

2.4. Compound 16a partially disrupts CNA – CF-PRIET interaction and inhibits NFATc activity in a dose-dependent manner while compounds of family 17 partially disrupt CNA – CF-PRIEIT and barely inhibit NFATc activity

Since only compounds of family **5** inhibit NFATc activity in a dose-dependent manner, to gain more insight regarding binding interactions and based on further modelling calculations, a novel set of compounds (**16a** and the small library of carboxamides **17c-e,g-i**) was designed (Fig. 5). Compound **16a** presents the same structure as carboxamide **6a** but bears a piperidinyl sulfonyl moiety instead of a methyl sulfonyl group at the west part of the molecule in an effort to increase hydrophobicity and aliphatic interactions towards the R332 area. The basic structure of the scaffold of **17** comes from compound **16a** but with a glycine unit joined to the sulfonyl group. The carboxyl group in series **17** was introduced to further strengthen polar interactions with either R332 or K100, two positively charged residues close to an extended polar subpocket (Fig. 2A–B) of the CN – PxIxIT peptide binding interface. Compounds **17c-e,g-i** consisted of an *N*-glycidyl sulfonyl moiety linked via an *N*-*m*-phenylamino-2-oxoethyl tether to different aromatic and heteroaromatic amides (3-methylthiophene, *p*-ethylphenyl, 3-benzothiophene, 2-quinoline, benzyloxy and *N*-methylaniline).

Compound **16a** was prepared following the three-step synthetic sequence used for family **6** (Supplementary Information, Scheme S1). The synthesis of carboxylic acids **17** began with the reaction of glycine *tert*-butyl ester **18** with nitrobenzenesulfonyl chloride **19** to afford sulfonamide **20** in almost quantitative yield (Scheme 3). *N*-Boc protection and subsequent nitro reduction delivered amine **22** which was coupled with *N*-benzyloxycarbonyl protected glycine **23** using EDCl·HCl along with HOBt to furnish **24** [30]. Then, hydrogenolysis led quantitatively to the common amine intermediate **25** which was coupled with the selected aromatic and heteroaromatic carboxylic acids **10c-e**,**h-i** using EDCl·HCl again. Finally, removal of the *tert*-butyl esters and carbamate protecting groups of **26** took place in a single step by treatment with TFA in CH_2Cl_2, thus providing the target compounds **17c-e**,**h-i**. Compound **17g** was prepared from **24** by treatment with TFA.

The competitive binding studies between the synthesized compounds and CF-PRIEIT to CNA, using the R3 peptide as a positive control, show that compounds **16a, 17c-e,g-i**, **5a** and **4** partially disrupt the CNA - CF-PRIEIT interaction in a fluorescence polarization assay in contrast to **6a** and **15** (Fig. 6A and B). The effect of compounds **16a** and **17c-e,g-i** on NFATc activity was also evaluated. HEK 293-T cells were treated with 50 and 10 μM of the given compounds and stimulated with Io + P. Compound **16a** markedly inhibited NFATc activity at 50 μM similar to compound **4**, however, compound family **17** inhibited NFATc activity much less efficiently at the same compound concentration (Fig. 6C). To better evaluate the effect of **16a** on NFATc activity, dose-response assays of the 3x-NFAT-luc reporter gene, the promoter activity of which is regulated by NFATc, were carried out. Compounds **5a** and in a lesser extent **16a**, but not **6a**, inhibit NFATc activity efficiently in a dose-dependent manner for concentrations ranging from 0.1 μM to 50 μM (Fig. 6D). These data suggest that newly synthesized compounds **16a** and family **17c-e,g-i** do not represent a substantial improvement as NFATc inhibitors compared to compounds of family **5**.

In order to visualize the potential elements of interaction with CNA, **16a** was also docked to CNA (Fig. 6E). Accordingly, the sulphone oxygen was observed to interact with Q333 *via* hydrogen bonding, as well as the amide NH atom to the M329 main chain carbonyl oxygen. The phenyl and indole groups occupied subpockets HYD1 and HYD2, forming hydrophobic interactions with I331, 288 and M290, and F299 and M329, respectively. The lack of a sulphonamide hydrogen bond donor is compensated by a possible polar interaction between the piperidine nitrogen atom and N330. Regarding compounds of series **17**, the addition of a carboxyl group to act as a hinge for a salt bridge with either R332 or K100 did not work as expected, probably by reducing the general hydrophobicity of the molecules, or by not being able to form strong polar contacts with these positively charged residues, as the latter are mostly exposed to a hydrophilic environment and spatially distant (Supplementary Information, Fig. S1).

2.5. Compounds 5a and 5e inhibit NFATc-dependent cytokine gene expression of primary human peripheral blood mononucleated cells, NFATc-dependent cytokine secretion and cell proliferation of activated human CD4$^+$ T cells

Once dephosphorylated, NFATcs at the nucleus bind DNA and, alone or in cooperation with other transcription factors, they induce the expression of NFATc-dependent genes, such as those encoding cytokines *IL2* and *IFNγ*. In this context, the abundance of the mRNAs of these genes was measured in human peripheral blood mononucleated cells (hPBMC) treated with compounds **5a**, **5e** and **4** at 50, 10 and 2 μM for 2 h and then stimulated with Io + P for 4 h. All the tested compounds inhibit gene expression of *IL2* and *IFNγ* in hPBMCs in a dose-dependent manner (Fig. 7A–B). Therefore, compounds **5a**, **5e** and **4** inhibit NFATc-mediated cytokine gene expression in a dose-dependent manner in human PBMCs.

Since compounds **5a, 5e** and **4** significantly inhibited the NFATc-dependent transcriptional activation of *IL2* and *IFNγ* genes, cytokine protein production was next measured in activated human CD4$^+$ T cells from hPBMCs Ca^{2+} stimulated with anti-CD3/anti-CD28 beads. Secretion of IL-2 protein by human CD4$^+$ cells was markedly reduced after **5a**, **5e** and **4** treatments, and in a lesser extent for IFNγ protein secretion, but not for the inhibitor of CN activity CsA (Fig. 7A–B). Furthermore, T cell

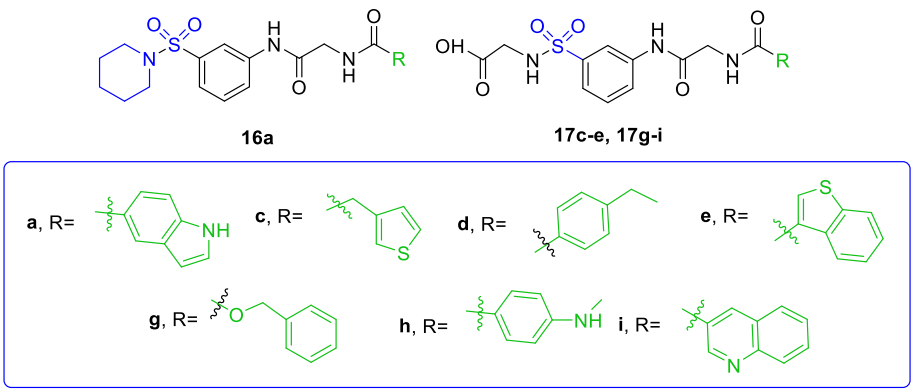

Fig. 5. Second-generation of CN-NFATc inhibitors.

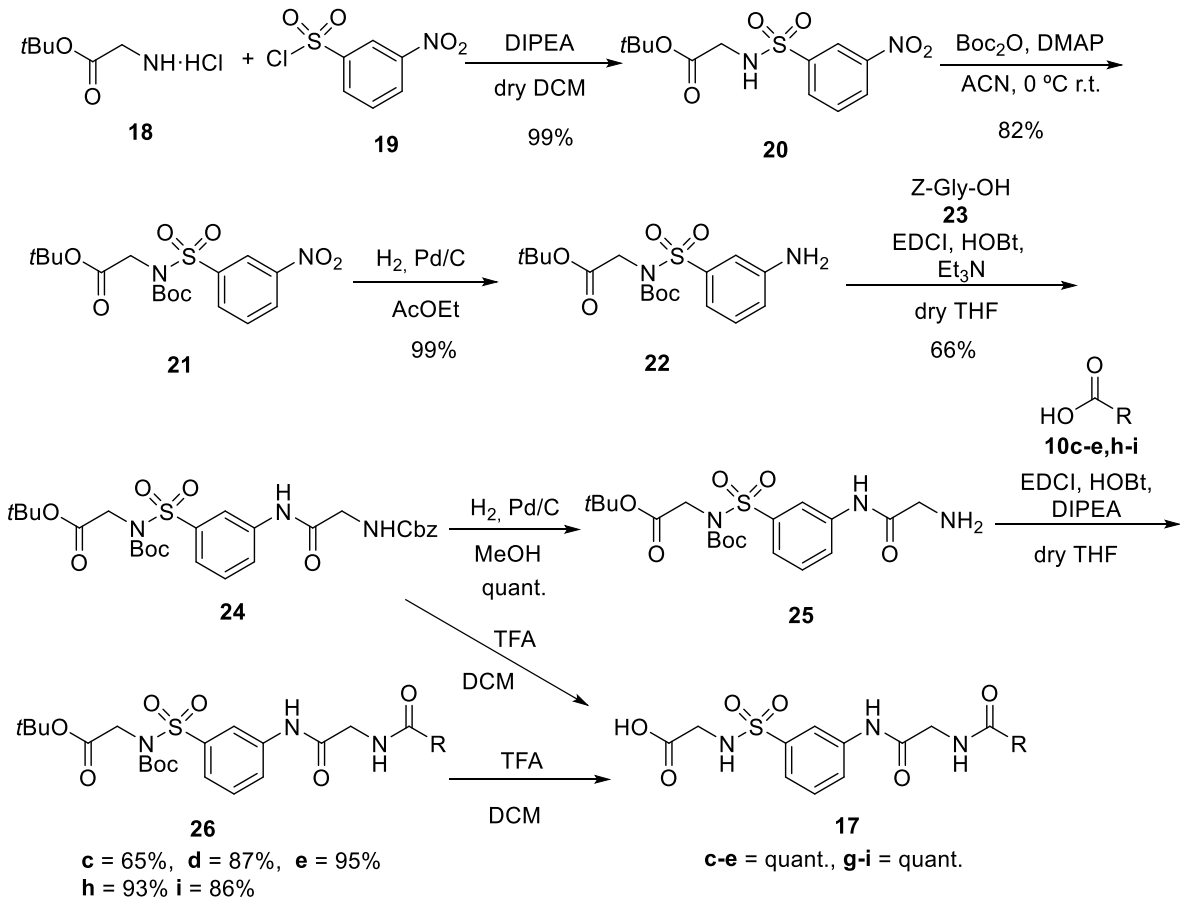

Scheme 3. Synthesis of compounds **17c-e,g-i**.

proliferation was also inhibited in a dose-dependent manner in cells treated with **5a, 5e** and **4** (Fig. 7C). Hence, compounds **5a, 5e** and **4** inhibit NFATc-dependent cytokine secretion and human T $CD4^+$ proliferation and therefore these compounds have immunosuppressant activity.

2.6. Compound 5a inhibits tumor growth and shows a tendency to reduce tumor angiogenesis in an orthotopic syngeneic model of TNBC

In order to assess the effect of the inhibitory compounds in an *in vivo* model, it was decided to determine whether these compounds were cytotoxic. In this context, several human and mouse normal and tumor cell lines were treated with 1 μM and 10 μM of compounds **5a**, **5e** and **4** for 72 h and cell viability was assessed using the CellTiter-Glo® Luminescent Cell Viability Assay (Promega). The tested compounds were not cytotoxic at 10 μM for any of the cell lines analyzed (Supplementary Information, Fig. S2).

Taking into account NFATc activity inhibition, two of the best compounds, **4** and **5a**, were selected to analyze their effect in *in vivo* experiments. Maximum tolerated doses (MTD) assay was performed to determine potential toxicity of **4** and **5a** compounds in BALB/c animals. Animals were administered a daily dose (Monday to Friday) by intraperitoneal injection with 50 mg/kg of each compound and killed at day seven. No macroscopic clinical signs of abnormal constitution, aberrant behavior, loss of weight or physical changes in general health conditions during the experiments were observed. No cytotoxic effects were observed at this concentration for compounds **4** and **5a** therefore it was decided to evaluate the effect of both compounds *in vivo*. Previous results have showed that inhibition of the CN-NFATc pathway is plausible for therapeutic intervention in triple negative breast cancer (TNBC), because of the role of this pathway in immune response, angiogenesis and tumor cell proliferation [4,31,32]. In addition, our group has shown that tumors overexpressing the RCAN3 protein or the RCAN3-derived R3 peptide inhibited NFATc signaling, and by these means impaired tumor progression and angiogenesis in a TNBC nude mice model [33]. Thus, the effect of both compounds **4** and **5a** on tumor angiogenesis in an orthotopic TNBC model using immunocompetent mice was evaluated by injection of mouse 4T1 TNBC cells. Briefly, 5×10^5 4T1 cells were injected into the left inguinal gland mammary fat pad BALB/c mice. When tumors reached a volume >100 mm^3 (at day 11 from cell injection), animals were treated daily (Monday to Friday) by intraperitoneal injection with 50 mg/kg of compounds **4**, **5a** or 5 mg/kg of FK506. Injection of 4T1 TNBC cells and intraperitoneal injection of compounds did not show a negative effect on body weight or general health conditions of mice with the exception of tumor growth.

Tumor weight of TNBC tumors after 15 days of treatment with **4**, **5a** or FK506 show a significant decrease compared to vehicle treatment (Fig. 8A), which suggests that these compounds affect TNBC tumor progression. TNBC tumors were excised at the experiment end point, fixed in 4% PFA, and paraffin-embedded histological sections were analyzed by immunohistochemistry (IHC) analysis with the endothelial cell marker CD31 antibody. Tumor angiogenesis in animals treated with compound **5a** showed a tendency to be reduced, $p = 0.0721$ (Fig. 8B). In contrast, tumor angiogenesis in animals treated with **4** was similar to control animals. FK506 significantly reduced tumor angiogenesis when compared to vehicle-treated mice (Fig. 8B). Therefore, compound **5a** reduces tumor growth and shows a tendency to reduce tumor angiogenesis in a syngeneic orthotopic model of TNBC.

3. Discussion

It is well established that cellular signaling of CN-NFATc is critical in

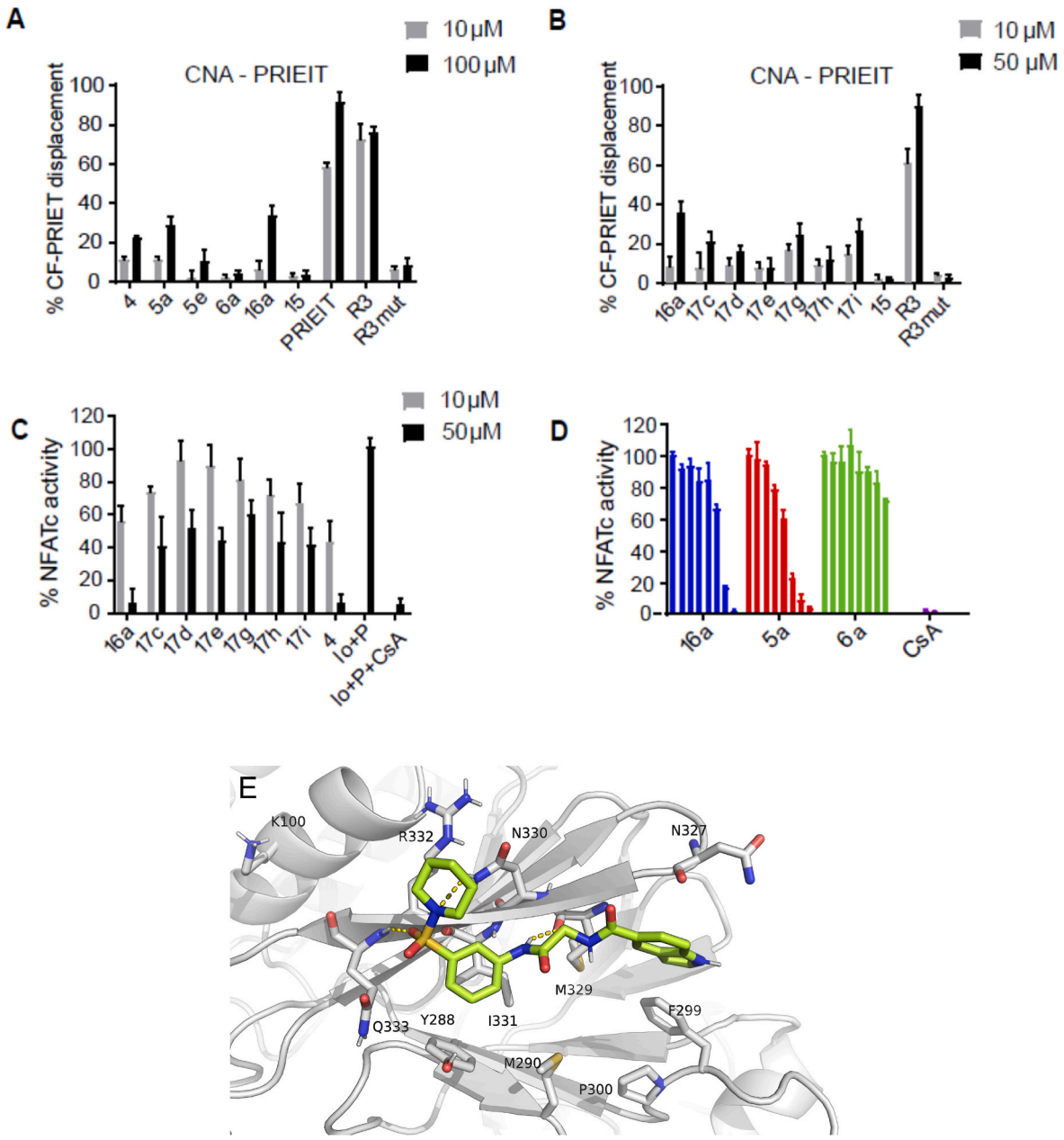

Fig. 6. Compound **16a** partially disrupts the CNA – CF-PRIET interaction and inhibits NFATc activity in a dose-dependent manner, while family **17** partially disrupts CNA – CF-PRIEIT and barely inhibits NFATc activity. **A** and **B:** The disruption of the interaction between CNA and the NFATc2-derived CF-PRIEIT peptide induced by the synthesized compounds was analyzed by fluorescence polarization analysis as described in Fig. 3A. R3 peptide was used as a positive control for interaction displacement. **C** and **D:** NFATc activity analysis using the 3xNFAT-luc reporter gene in HEK 293-T cells was performed as described in Fig. 4B. Cells were treated with each compound at 10 µM and 50 µM on panel **C** and at 0/0.1/0.5/2/5/10/20/50 µM (represented from left to right on the graph) on panel **D**. **E:** Predicted **16a** (shown in light green) – CNA (shown in grey) interaction. Hydrogen bonds are depicted in yellow dashed lines.

the regulation of biological processes such as the immune response, angiogenesis, development, and growth [3–5]. Therefore, deregulation of this signaling pathway causes pathophysiological disorders such as carcinogenesis and metastasis. In cancer, the pathology is not caused by DNA mutations but by an increase in the abundance and/or the activity of the CN-NFATc signaling pathway [4]. It has been reported that patient biopsies of TNBC tumors show overproduction of NFATc and/or over-activation of NFATc-mediated gene expression in different cellular programs [31,32] such as cell survival, proliferation, migration, and cell invasion and tumor angiogenesis [34]. Therefore, inhibition of the CN-NFATc pathway has been suggested as plausible for therapeutic intervention in cancer [32,35]. Furthermore, the discovery of the PxIxIT sequence of NFATcs as the main anchoring sequence for binding to CN, of the LxVP motif, as a substrate binding site to CN, and of both motifs as responsible for NFATc cellular signaling, was crucial in understanding the molecular mechanisms underlying pathophysiological processes where the CN-NFATc pathway is exacerbated, such as in TNBC. Several substrates, inhibitors and regulators of CN have also been described to exhibit PxIxIT and/or LxVP motifs, which allow them to compete with NFATc for binding to CN and block cellular signaling of these transcription factors [6,8,9]. Identifying selective CN-NFATc inhibitors that mimic the functional effect of these PxIxIT and LxVP SLiMs could be valuable as therapeutic target tools but also for mechanistically elucidating the involvement of this signaling pathway in TNBC development.

Several approaches have been undertaken by several research groups to identify molecules that could inhibit the CN-NFATc signaling

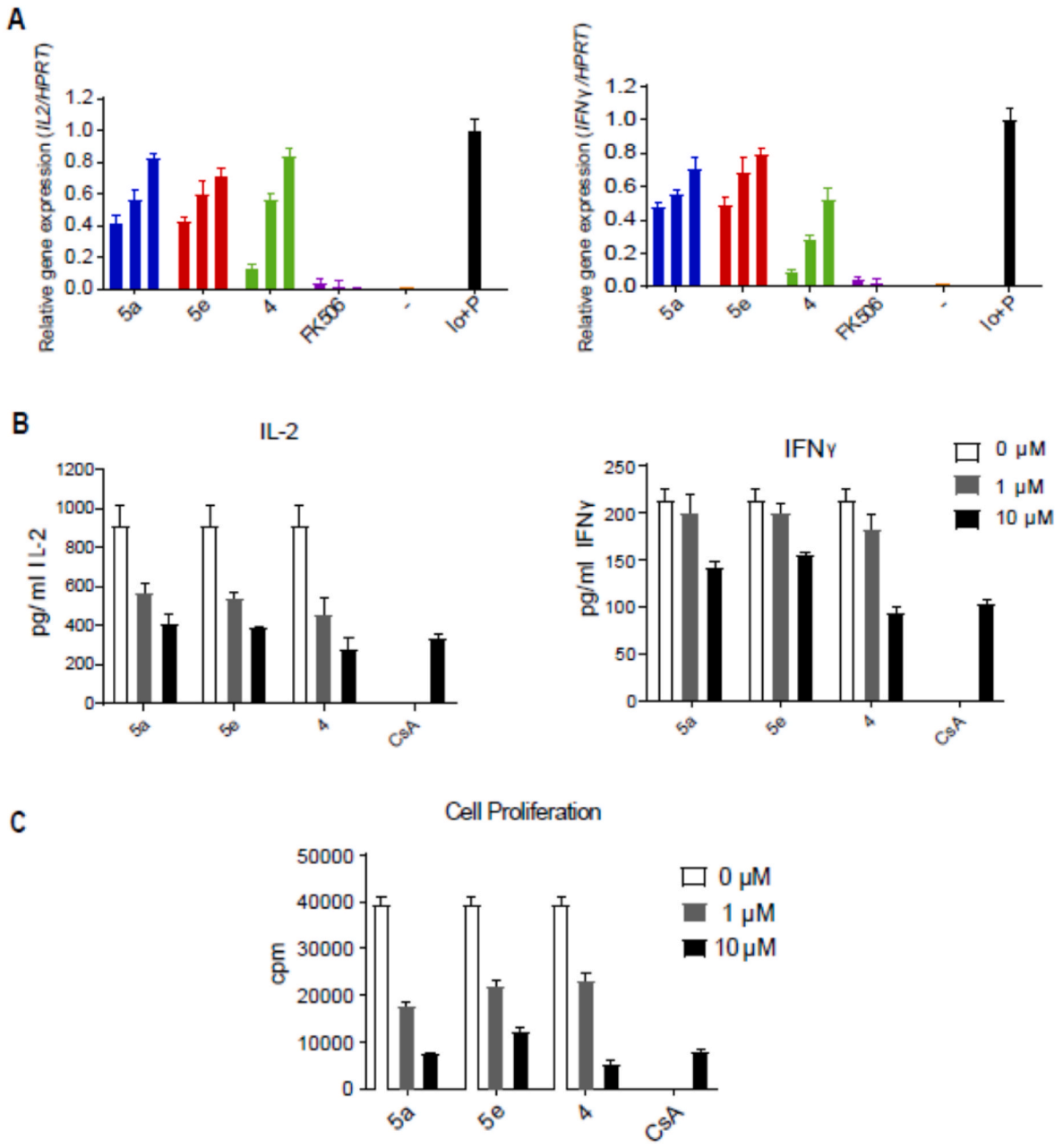

Fig. 7. Compounds **5a** and **5e** inhibit NFATc-dependent cytokine gene expression of human PMBCs, NFATc-dependent cytokine secretion and cell proliferation of activated human $CD4^+$ T cells. **A:** Inhibition of NFATc-dependent gene expression by the selected compounds was assessed through real time PCR for *IL2* (left) and *IFNγ* (right) cytokine genes relative to the human *HPRT* housekeeping gene. Isolated hPMBC were treated with each compound at 50 μM, 10 μM and 2 μM for 2 h and, without removing it, calcium stimulated with Io + P for 4 h, as described in Fig. 4B. The ΔΔCT method was used to determine the fold change for gene expression. Data corresponds to the mean ± SD of 3 independent experiments with triplicates. FK506 was used as a positive control for CN activity inhibition. The unstimulated cells control is shown as a black dash. **B:** Compound inhibition of NFATc-mediated IL-2 and IFNγ secretion by activated human $CD4^+$T cells. Cells were treated with each compound at 10 μM and 1 μM for 2 h and, in the presence of this, calcium stimulated by co-stimulation with anti-CD3 and anti-CD28 antibodies for 48 h. NFATc-dependent IL-2 and IFNγ production were assessed in cell culture media from $CD4^+$ cells *via* enzyme-linked immunosorbent assay (ELISA). Data is given as mean ± SEM. **C:** Inhibition of activated $CD4^+$T cells proliferation measured at 72 h by [^{3}H]-thymidine incorporation on DNA.

pathway as an alternative to current immunosuppressant drugs CsA and FK506, which unfortunately cause severe side effects after long-term treatment. Among the molecules identified so far, the most successful has been the NFATc-derived PRIEIT peptide, the sequence of which has been optimized to the VIVIT peptide for binding with higher affinity to CNA [36]. Taking this into account and based on the previously described small non-peptidic compounds **3** and **4** [25], we have synthesized and studied the functionality of several families of molecules which mimic the CN-binding PxIxIT sequence IAITT of the scaffold AKAP79 protein for binding to CN and for inhibiting CN-NFATc cell signaling [15].

The novel compounds present a sulfonamide (compounds of families **5** and **17** and **16a**), or a sulfone group (compounds of family **6**) linked *via* different tethers to several aromatic and heteroaromatic amides. Our results show that most of the compounds in families **5** and **17** and compound **16a** partially disrupt the interaction between CNA and the NFATc2-derived PRIET peptide, which is crucial for NFATc cell signaling. In contrast, the carboxamide compounds from family **6** do not compete with the CNA – CF-PRIET interaction. Moreover, most of the compounds from family **5** and compound **16a** inhibit NFATc activity in

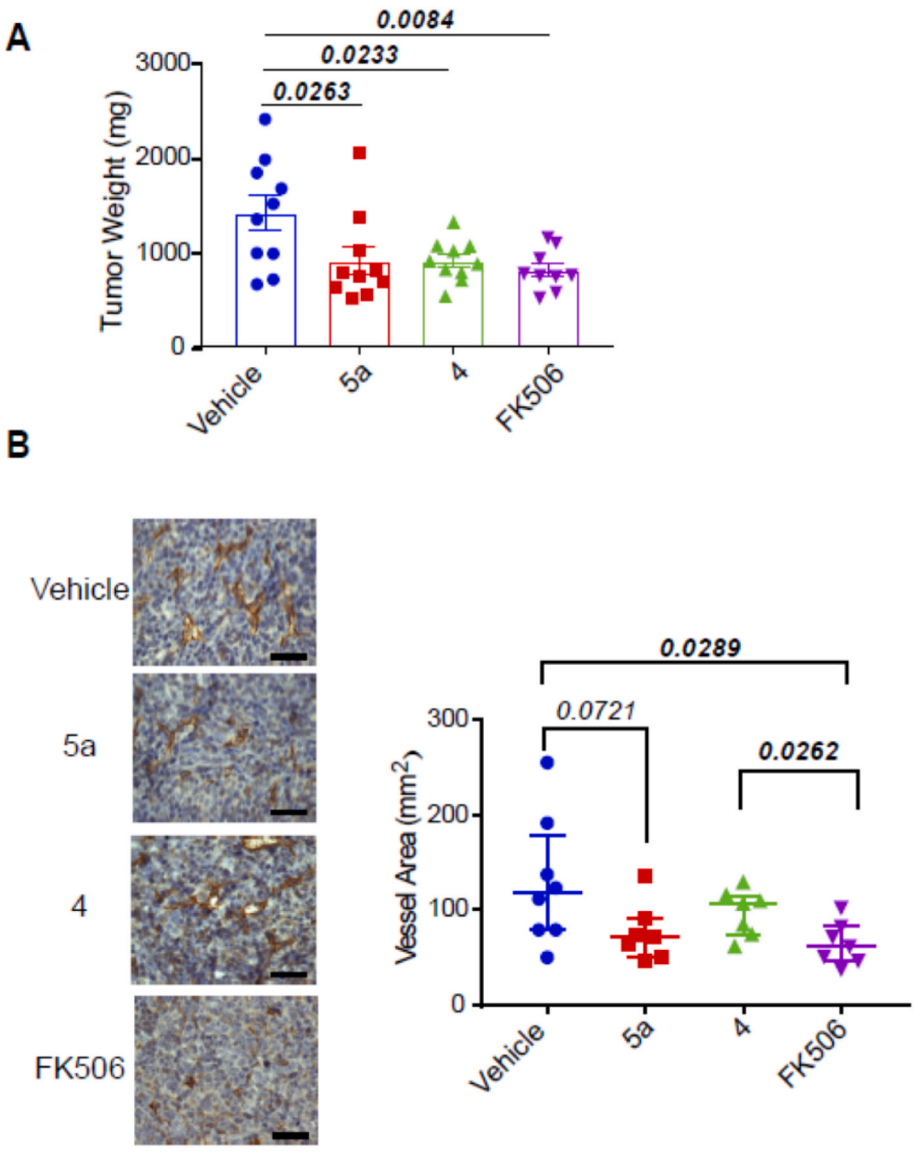

Fig. 8. The novel non-peptide compound **5a** inhibits tumor growth and shows a tendency to reduce tumor angiogenesis in an orthotopic syngeneic model of TNBC. **A:** Mice were injected with 5×10^5 transduced 4T1 cells into the mammary fat pad (10 animals for each experimental group). When tumors reached a volume >100 mm^3 (at day 11 from cell injection), animals were treated by intraperitoneal injection with 50 mg/kg of compounds **4**, **5a** or 5 mg/kg of FK506. FK506 was used as a control inhibitor of CN phosphatase activity. Animals were euthanized 15 days post treatment and tumor weight was measured. The weights of the tumors of each experimental group are represented as mean ± SEM. Statistical analysis was performed using One-way ANOVA with Dunnett's post-hoc test. Significance is shown as bold characters. **B:** Left panel: Representative images of histologic sections stained with rabbit anti-CD31 of TNBC mice treated with vehicle or compounds **5a**, **4** or FK506. Histological sections were counterstained with hematoxylin (blue). Brown color indicates $CD31^+$ endothelial cells. Scale bars represent 200 μm. Right panel: Quantification of mean vessel area/mm^2 per high power field (HPF). Statistical analysis was performed using the Mann-Whitney test (*p* values that are less than 0.1 are specified on the graph). Data is presented as median ± interquartile range.

Ca^{2+} stimulated cells with a similar efficacy to compound **4**. However, compounds of family **17** inhibit NFATc activity with much lower efficiency. Interestingly, compounds of family **6** failed to inhibit NFATc activity in Ca^{2+} stimulated cells. This data suggests that a sulfonamide group is important for NFATc inhibitory activity, while the presence of the glycine unit joined to the sulfonyl group on compounds **17** is detrimental for NFATc inhibitory activity.

From all the synthesized compounds, carboxamides **5a**, **5e** and **16a** are the most effective molecules which bind to CN and inhibit CN-NFATc signaling. In particular, **5a** is the best compound and our docking calculations demonstrate that it binds to CNA in a similar manner to the proposed binding of compound **4**, sharing all the crucial interactions as well as an additional potential hydrogen bond with N327.

Ligand binding and subsequent activation of T-cell receptors (TCR) causes T-cell activation, CN-NFATc signaling activation, and posterior transcriptional induction of NFATc-dependent gene expression, followed by production of cytokines and chemokines [37,38]. Cytokines such as IL-2 and IFNγ are important mediators in the regulation of the immune response. In this context, compounds **5a** and **5e** impair NFATc-dependent gene expression in activated hPBMCs or $CD4^+$ T cells as observed by a decrease of mRNA and protein levels of IL2 and IFNγ, and consequently, these compounds have immunosuppressant activity. Furthermore, compounds from family **5** do not affect the CNA enzymatic activity towards the pNPP substrate. Unlike these compounds, the immunosuppressive drugs CsA and FK506, used to avoid acute graft rejection, inhibit CN phosphatase activity toward all CN substrates, which causes severe side effects that prevent their long-term administration [23]. Therefore, our small compounds **5a** and **5e** that bind to CNA and inhibit NFATc cell signaling in activated human $CD4^+$ lymphocytes without affecting CN phosphatase activity are valuable tools for immunosuppressive therapy as they could substantially decrease CN-immunosuppressant side effects.

Overexpression of the endogenous modulator RCAN3 protein and of the RCAN3- derived R3 peptide strongly decreases tumor growth progression, angiogenesis and tumor neutrophil infiltration in an orthotopic model of TNBC in athymic nude mice [33]. It is well known that triple negative breast cancer is a heterogeneous disease characterized by the lack of druggable targets [39]. Angiogenesis is an important factor in TNBC progression. TNBC tumors show high intratumoral microvessel density [41] and express high levels of vascular endothelial growth factor (VEGF) [40]. Several reports have shown that NFATc inhibition renders an impaired angiogenic response *in vivo*. For instance, administration of the CN inhibitors CsA and FK506 has been shown to effectively impair the angiogenic response elicited by VEGF in endothelial

cells *in vivo* [42,43]. Opposite results have also been reported [44], where NFATc activate cell signaling in MDA-MB-231 cells but suppresses xenograft TNBC tumor growth.

With this precedent, the effect of our best candidate, **5a**, was analyzed in a syngeneic orthotopic TNBC mouse model along with compounds **4** and FK506. Tumor weight after 15 days of treatment with **4**, **5a** or FK506 is significantly reduced compared to vehicle treatment. In addition, the quantification of vessel area density on histological sections using IHC analyzed with anti-CD31 showed a clear tendency of reduced tumor angiogenesis in mice treated with compound **5a** in comparison to mice treated with vehicle. Surprisingly, compound **4** had no effect on tumor angiogenesis while FK506 significantly reduced it. This difference in the functional effect on tumor angiogenesis between compounds **5a** and **4** could be explained by the potential additional polar contact that **5a** could establish with N327 in CNA, but we cannot rule out other possibilities such as different bioavailability of both compounds, though this remains to be analyzed. In addition, a stronger administration regimen of compound **5a** could be envisaged and/or the use of nanocarriers to target the tumors [45,46]. Therefore, it becomes evident that compound **5a**, which inhibits CN-NFATc signaling *in vitro*, has immunosuppressant activity and is able to reduce tumor weight and tumor angiogenesis *in vivo* even in the presence of a totally functional immune system. These findings may constitute a novel therapeutic approach against pathologies without targeted therapy and with an exacerbated NFATc signaling pathway such as TNBC.

In summary, the discovery of specific CN-NFAT inhibitors as alternative immunosuppressants to CsA and FK506 that may be more effective in diseases with aberrant CN-NFATc signaling, such as TNBC, while exhibiting fewer secondary effects, would lead to more efficient combined therapies for the treatment of these diseases with improved clinical tolerance. We consider that there is sufficient basis to propose the selective inhibition of the CN-NFATc signaling pathway as a valuable therapeutic strategy to be more efficient and with less associated side effects on diseases with aberrant CN-NFATc signaling. In fact, the use of peptides including the PxIxIT sequence itself would be the first option. Although this approach should not be dismissed, it must be acknowledged that it would be a highly expensive treatment with the inconvenience associated to the known oral absorption and pharmacokinetic problems derived from the administration of proteins.

Based on previously identified compounds through a pharmacophore-based virtual screening and using docking calculations, we have designed and synthesized several families of compounds which mimic the PxIxIT sequence binding to CNA and inhibit CN-NFATc cell signaling – these compounds have the potential to be used as immunosuppressive drugs.

Our docking calculations demonstrate that, from all the prepared compounds, carboxamide **5a** binds to CNA in similar manner to the proposed binding of compound **4**, sharing all the crucial interactions as well as an additional potential polar contact with N327. This new non-peptide small ligand binds to CNA *in vitro* and inhibits CN-NFATc signaling without interfering with CN phosphatase activity. Moreover, **5a** inhibits cytokine mRNA production in activated hPBMC and cytokine secretion and cell proliferation in activated $CD4^+$ T cells, indicating that it has therapeutic potential as an immunosuppressant. Finally, compound **5a** also reduces TNBC tumor weight and shows a tendency to reduce tumor angiogenesis in an immunocompetent model of TNBC, suggesting that **5a** has anti-tumor progression potential. All in all, **5a** has been validated as an agent with therapeutic potential against CN-NFATc signaling, and as a tool that can be further utilized in drug development.

3.1. Experimental

General procedures. Materials and methods: Commercially available reagents were used as received. Solvents were dried by distillation over the appropriate drying agents. All reactions were monitored by analytical thin-layer chromatography (TLC) using silica gel 60 precoated aluminum plates (0.20 mm thickness). Flash column chromatography was performed using silica gel Geduran® SI 60 (40–63 μm). ^{1}H NMR and ^{13}C NMR spectra were recorded at 250, 360, 400 MHz and 90, 100 MHz, respectively. Proton chemical shifts are reported in ppm (δ) ($CDCl_3$, δ 7.26 or CD_3OD, δ 3.31). Carbon chemical shifts are reported in ppm (δ) ($CDCl_3$, δ 77.16 or CD_3OD, δ 49.00). NMR signals were assigned with the help of HSQC. Infrared peaks are reported in cm^{-1}. The purity of the tested compounds was determined to be over 95% by HPLC analysis (see the Supplementary Material). Melting points were determined on hot stage and are uncorrected. HRMS were recorded using electrospray ionization (ESI).

***N*-(3-Nitrobenzyl)methanesulfonamide, 8.** To a solution of 3-nitrobenzylamine hydrochloride, **7**, (730 mg, 3.87 mmol) in CH_2Cl_2 (25 mL), Et_3N (1.1 mL, 7.74 mmol) and MsCl (0.32 mL, 4.06 mmol) were sequentially added. The mixture was stirred at rt for 10 min. Then, the reaction was quenched with water (25 mL), and the layers were separated. The organic layer was washed with brine (2 x 25 mL), dried over anhydrous $MgSO_4$ and concentrated under reduced pressure to obtain sulphonamide **8** as a yellow solid (864 mg, 3.75 mmol, 98% yield). Mp = 75–78 °C (from CH_2Cl_2). ^{1}H NMR (400 MHz, acetone-d_6) δ 8.30 (s, 1H, H-2), 8.16 (d, $J_{4,5}$ = 7.9 Hz, 1H, H-4), 7.87 (d, $J_{6,5}$ = 7.9 Hz, 1H, H-6), 7.67 (t, $J_{5,4} = J_{5,6}$ = 7.9 Hz, 1H, H-5), 6.74 (br s, 1H, CH_2NH), 4.50 (d, $J_{CH2,CH2NH}$ = 6.5Hz, 2H, -CH_2-), 2.97 (s, 3H, -CH_3); ^{13}C NMR (100.6 MHz, acetone-d_6) δ 149.3 (C_3), 142.0 (C_1), 134.9 (C_5), 130.6 (C_6), 123.2 (C_2), 123.0 (C_4), 46.6 (-CH_2-), 40.5 (-SO_2CH_3); IR (ATR) 3231, 1527, 1352, 1300, 1138 cm^{-1}. HRMS (ESI+) calcd. for $[C_8H_{10}N_2O_4S+Na]^+$ $[M+Na]^+$: 253.0259; found: 253.0254.

***N*-(3-Aminobenzyl)methanesulfonamide, 9.** A mixture of compound **8** (830 mg, 3.61 mmol) and 10% Pd/C (83 mg) in EtOAc (11 mL) was stirred under H_2 (1 atm) overnight. The suspension was filtered over Celite® and the filtrate was concentrated to obtain **9** as a brown solid (718 mg, 3.59 mmol, 99% yield). Mp = 69–71 °C (from CH_2Cl_2). ^{1}H NMR (400 MHz, DMSO-d_6) δ 7.42 (t, $J_{SO2NH,CH2}$ = 6.2 Hz, 1H, –SO_2NH-), 6.98 (t, $J_{5,4} = J_{5,6}$ = 7.6 Hz, 1H, H-5), 6.55 (s, 1H, H-2), 6.49 - 6.45 (m, 2H, H-4, H-6), 5.06 (br s, 2H, –NH_2), 3.99 (d, $J_{CH2,NHSOO}$ = 6.2 Hz, 2H, -CH_2-), 2.82 (s, 3H, -CH_3); ^{13}C NMR (62.5 MHz, DMSO-d_6): δ 148.3 (C_3), 138.7 (C_1), 128.9 (C_5), 115.5 (C_6), 113.4 (C_2), 113.2 (C_4), 46.4 (-CH_2-), 40.0 (-SO_2CH_3); IR (ATR) 3416, 3328, 3037, 2847, 1593, 1465, 1299, 1141 cm^{-1}. HRMS (ESI+) calcd. for $[C_8H_{12}N_2O_2S+H]^+$ $[M+H]^+$: 201.0698; found: 201.0695.

***N*-(3-{ [(Methylsulfonyl)amino] methyl}phenyl)-*1H*-indole-5-carboxamide, 5a.** To a stirred solution of amine **9** (229 mg, 1.14 mmol) in dry THF (10 mL) under N_2 atmosphere, a solution of indole-5-carboxylic acid, **10a**, (276 mg, 1.72 mmol), EDCI (0.30 mL, 1.71 mmol), HOBt (231 mg, 1.71 mmol) and DIPEA (1.00 mL, 5.74 mmol) in dry THF (10 mL) was added. The reaction mixture was stirred overnight at rt. Then, the reaction was quenched with water (10 mL) and extracted with EtOAc (10 mL). The organic layer was washed with water (3 x 10 mL), dried over anhydrous Na_2SO_4 and concentrated *in vacuo*. Purification by column chromatography (CH_2Cl_2/MeOH, 30:1) afforded compound **5a** as a white solid (318 mg, 0.93 mmol, 81% yield). Mp = 89–90 °C (from acetone). ^{1}H NMR (400 MHz, DMSO-d_6) δ 11.41 (s, 1H, -N*H*-), 10.16 (s, 1H, -CON*H*-), 8.27 (s, 1H, H-4), 7.83 (s, 1H, H-2′), 7.73 (m, 2H, H-6, H-6′), 7.59 (t, $J_{CH2NH,CH2}$ = 6.4 Hz, 1H, –CH_2NH-), 7.49 - 7.46 (m, 2H, H-2, H-7), 7.31 (t, $J_{5',4'} = J_{5',6'}$ = 7.8 Hz, 1H, H-5′), 7.05 (d, $J_{4',5'}$ = 7.8 Hz, 1H, H-4′), 6.58 (s, 1H, H-3), 4.15 (d, $J_{CH2,CH2NH}$ = 6.4 Hz, 2H, -CH_2-), 2.89 (s, 3H, -SO_2CH_3); ^{13}C NMR (100.6 MHz, DMSO-d_6) δ 166.5 (-*C*ONH-), 139.8 ($C_{1'}$), 138.6 ($C_{3'}$), 137.6 (C_{7a}), 128.5 ($C_{5'}$), 127.0 (C_{3a}/C_5), 126.9 (C_2), 125.7 (C_{3a}/C_5), 122.4 ($C_{4'}$), 121.0 (C_6), 120.5 (C_4), 119.5 ($C_{6'}$), 119.1 ($C_{2'}$), 111.1 (C_7), 102.2 (C_3), 46.2 (CH_2NH), 40.0 (-SO_2CH_3); ^{13}C NMR (100.6 MHz, acetone-d_6) δ 167.4 (-*C*ONH-), 141.1 ($C_{1'}$), 139.7 ($C_{3'}$), 139.0 (C_{7a}), 129.6 ($C_{5'}$), 129.6 (C_{3a}/C_5), 128.5 (C_2), 127.3 (C_{3a}/C_5), 123.5 ($C_{4'}$), 121.9 (C_6), 121.3 (C_4), 120.3 ($C_{6'}$), 120.0 ($C_{2'}$), 111.9 (C_7), 103.5 (C_3), 47.7 (CH_2NH), 40.6 (-SO_2CH_3); IR (ATR) 3291, 1611, 1540, 1436, 1310, 1146 cm^{-1}. HRMS (ESI+) calcd. for $[C_{17}H_{17}N_3O_3S+H]^+$ $[M+H]^+$: 344.1069; found: 344.1065. HPLC purity:

98.27%.

***N*-(3-{ [(Methylsulfonyl)amino] methyl}phenyl)-2-naphthamide, 5b.** Compound **5b** was prepared as described for **5a** by using a solution of compound **9** (58 mg, 0.29 mmol) in dry THF (2 mL) and a solution of commercially available 2-naphtoic acid, **10b**, (75 mg, 0.44 mmol), EDCI (80 μL, 0.44 mmol), HOBt (60 mg, 0.44 mmol) and DIPEA (200 μL, 1.16 mmol) in dry THF/DMF (3 mL/2 mL). The residue was purified by recrystallization in Et_2O to furnish product **5b** as a white solid (88 mg, 0.26 mmol, 88% yield). Mp = 178–183 °C (from acetone). ^{1}H NMR (400 MHz, DMSO-d_6) δ 10.47 (s, 1H, CON*H*), 8.59 (s, 1H, H-1), 8.10 - 8.00 (m, 4H, H_3/H_4/H_5/H_6/H_7/H_8), 7.84 (s, 1H, H-2′), 7.76 (d, $J_{6',5'}$ = 7.9 Hz, 1H, H-6′), 7.67 - 7.59 (m, 3H, H_5/H_6/H_7/H_8/CH_2N*H*), 7.36 (t, $J_{5',4'} = J_{5',6'}$ = 7.9 Hz, 1H, H-5′), 7.11 (d, $J_{4',5'}$ = 7.9 Hz, 1H, H-4′), 4.18 (d, $J_{CH2,NHCH2}$ = 6.3 Hz, 2H, -C*H*$_2$-), 2.90 (s, 3H, -SO_2CH_3); ^{13}C NMR (100.6 MHz, DMSO-d_6) δ 165.6 (-*C*ONH-), 139.3 ($C_{1'}$), 138.8 ($C_{3'}$), 134.3 (C_2), 132.2 (C_{4a}/C_{8a}), 132.1 (C_{4a}/C_{8a}), 128.9/128.0/127.8/127.7/126.8/124.4 (C_1/C_3/C_4/C_5/C_6/C_7/C_8), 128.7 ($C_{5'}$), 123.0 ($C_{4'}$), 119.6 ($C_{2'}$), 119.3 ($C_{6'}$), 46.1 (*C*H_2NH), 40.0 (-SO_2CH_3); IR (ATR) 3207, 1645, 1543, 1437, 1302, 1130 cm^{-1}. HRMS (ESI+) calcd. for [$C_{19}H_{18}N_2O_3S$+H]$^+$ [M+H]$^+$: 355.1116; found: 355.1112.

***N*-(3-{ [(Methylsulfonyl)amino] methyl}phenyl)-2-(3-thienyl) acetamide, 5c.** Compound **5c** was prepared as described for **5a** by using a solution of compound **9** (64 mg, 0.32 mmol) in dry THF (3 mL) and a solution of commercially available 3-thiopheneacetic acid, **10c**, (68 mg, 0.48 mmol), EDCI (85 μL, 0.48 mmol), HOBt (65 mg, 0.48 mmol) and DIPEA (220 μL, 1.28 mmol) in dry THF/DMF (3 mL/1 mL). The residue was purified by recrystallization in Et_2O to furnish product **5c** as a white solid (65 mg, 0.20 mmol, 63% yield). Mp = 153–157 °C (from acetone). ^{1}H NMR (400 MHz, DMSO-d_6) δ 10.16 (s, 1H, CON*H*), 7.58 - 7.52 (m, 3H, H-6″, H-2″, CH_2N*H*), 7.48 (m, 1H, H-5′), 7.32 (m, 1H, H-2′), 7.26 (t, $J_{5'',4''} = J_{5'',6''}$ = 7.8 Hz, 1H, H-5″), 7.09 (dd, $J_{4',5'}$ = 4.9 Hz, $J_{4',2'}$ = 1.1 Hz, 1H, H-4′), 7.01 (d, $J_{4'',6''}$ = 7.8 Hz, 1H, H-4″), 4.11 (d, $J_{NHCH2,CH2}$ = 6.4 Hz, 2H, NHC*H*$_2$), 3.65 (s, 2H, H-2), 2.86 (s, 3H, -SO_2CH_3); ^{13}C NMR (100.6 MHz, DMSO-d_6): δ 168.7 (*C*ONH), 139.3 ($C_{1''}$), 138.9 ($C_{3''}$), 135.6 ($C_{3'}$), 128.7 ($C_{4'}$/$C_{5''}$), 128.7 ($C_{4'}$/$C_{5''}$), 125.8 ($C_{5'}$), 122.5 ($C_{4''}$, $C_{2'}$), 118.3 ($C_{2''}$/$C_{6''}$), 118.0 ($C_{2''}$/$C_{6''}$), 46.0 (*C*H_2NH), 39.9 (-SO_2CH_3), 38.1 (C_2); IR (ATR) 3259, 1657, 1535, 1309, 1147 cm^{-1}. HRMS (ESI+) calcd. for [$C_{14}H_{16}N_2O_3S_2$+Na]$^+$ [M+Na]$^+$: 347.0500; found: 347.0495.

4-Ethyl-*N*-(3-{ [(methylsulfonyl)amino] methyl}phenyl)benzamide, 5d. Compound **5d** was prepared as described for **5a** by using a solution of compound **9** (66 mg, 0.32 mmol) in dry THF (3 mL) and a solution of commercially available 4-ethylbenzoic acid, **10d**, (72 mg, 0.48 mmol), EDCI (85 μL, 0.48 mmol), HOBt (65 mg, 0.48 mmol) and DIPEA (220 μL, 1.28 mmol) in dry THF/DMF (3 mL/1 mL). The residue was purified by recrystallization in Et_2O to furnish product **5d** as a white solid (50 mg, 0.15 mmol, 47% yield). Mp = 145–149 °C (from acetone). ^{1}H NMR (400 MHz, DMSO-d_6) δ 10.19 (s, 1H, CON*H*), 7.90 (d, $J_{2,3} = J_{6,5}$ = 8.3 Hz, 2H, H-2, H-6), 7.79 (s, 1H, H-2′), 7.70 (m, $J_{6',5'}$ = 8.0 Hz, 1H, H-6′), 7.57 (t, $J_{CH2NH,CH2}$ = 6.4 Hz, 1H, CH_2N*H*), 7.36 (d, $J_{3,2} = J_{5,6}$ = 8.3 Hz, 2H, H-3, H-5), 7.32 (t, $J_{5',4'} = J_{5',6'}$ = 7.9 Hz, 1H, H-5′), 7.08 (d, $J_{5',6'}$ = 7.9 Hz, 1H, H-4′), 4.15 (d, $J_{CH2,CH2NH}$ = 6.3 Hz, 2H, -NHC*H*$_2$-), 2.88 (s, 3H, -SO_2CH_3), 2.69 (q, $J_{CH2,CH3}$ = 7.6 Hz, 2H, -C*H*$_2$CH$_3$), 1.22 (t, $J_{CH3,CH2}$ = 7.6 Hz, 3H, -CH_2CH_3); ^{13}C NMR (100.6 MHz, DMSO-d_6): δ 165.4 (*C*ONH), 147.7 (C_4), 139.3 ($C_{1'}$), 138.7 ($C_{3'}$), 132.3 (C_1), 128.5 ($C_{5'}$), 127.7 (C_2, C_6), 127.7 (C_3, C_5), 122.8 ($C_{4'}$), 119.5 ($C_{2'}$), 119.2 ($C_{6'}$), 46.1 (*C*H_2NH), 40.0 (-SO_2CH_3), 28.0 (-*C*H_2CH$_3$), 15.4 (-CH_2CH_3). IR (ATR): 3263, 2966, 1645, 1538, 1307, 1144 cm^{-1}. HRMS (ESI+) calcd. for [$C_{17}H_{20}N_2O_3S$+H]$^+$ [M+H]$^+$: 333.1273; found: 333.1267.

***N*-(3-{ [(Methylsulfonyl)amino] methyl}phenyl)-1-benzothiophene-3-carboxamide, 5e.** Compound **5e** was prepared as described for **5a** by using a solution of compound **9** (295 mg, 1.47 mmol) in dry THF (10 mL) and a solution of commercially available benzothiophene-3-carboxylic acid, **10e**, (399 mg, 2.24 mmol), EDCI (0.40 mL, 2.26 mmol), HOBt (302 mg, 2.23 mmol) and DIPEA (1.10 mL, 6.31 mmol) in dry THF (10 mL). The residue was purified by recrystallization in CH_2Cl_2 to furnish product **5e** as a white solid (399 mg, 1.11 mmol, 75% yield). Mp = 139–140 °C (from acetone). ^{1}H NMR (360 MHz, DMSO-d_6) δ 10.39 (s, 1H, -CON*H*-), 8.57 (s, 1H, H-2), 8.42 (d, $J_{4,5}$ = 7.5 Hz, 1H, H-4), 8.08 (d, $J_{7,6}$ = 7.6 Hz, 1H, H-7), 7.80 (s, 1H, H-2′), 7.70 (d, $J_{6',5'}$ = 8.0 Hz, 1H, H-6′), 7.61 (t, $J_{NHCH2,CH2}$ = 6.3 Hz, 1H, CH_2N*H*), 7.51 - 7.43 (m, 2H, H-5, H-6), 7.35 (t, $J_{5',4'} = J_{5',6'}$ = 8.0 Hz, 1H, H-5′), 7.09 (d, $J_{4',5'}$ = 8.0 Hz, 1H, H-4′), 4.17 (d, $J_{CH2,CH2NH}$ = 6.3 Hz, 2H, -C*H*$_2$-), 2.90 (s, 3H, -SO_2CH_3); ^{13}C NMR (100.6 MHz, DMSO-d_6) δ 161.9 (*C*ONH), 139.4 (C_{3a}/C_{7a}), 139.2 ($C_{3'}$), 138.9 ($C_{1'}$), 137.1 (C_{3a}/C_{7a}), 131.9 (C_2), 131.0 (C_3), 128.7 ($C_{5'}$), 125.0 (C_5, C_6), 124.3 (C_4), 122.9 (C_7, $C_{4'}$), 119.4 ($C_{6'}$) 119.1 ($C_{2'}$), 46.1 (–CH_2–), 39.9 (SO_2CH_3); IR (ATR) 3250, 1643, 1543, 1420, 1305, 1149 cm^{-1}. HRMS (ESI+) calcd. for [$C_{17}H_{16}N_2O_3S_2$+Na]$^+$ [M+Na]$^+$: 383.0500; found: 383.0497. HPLC purity: 98.10%.

***N*-(3-(Methylsulfonamidomethyl)phenyl)benzo [b] thiophene-5-carboxamide, 5f.** Compound **5f** was prepared as described for **5a** by using a solution of compound **9** (34 mg, 0.17 mmol) in dry THF (2 mL) and a solution of commercially available 1-benzothiophene-5-carboxylic acid, **10f**, (25 mg, 0.14 mmol), EDCI (24 μL, 0.15 mmol), HOBt (21 mg, 0.15 mmol) and DIPEA (100 μL, 0.56 mmol) in dry THF/DMF (2 mL/1 mL). The residue was purified by recrystallization in Et_2O to furnish product **5f** as a white solid (26 mg, 72 μmol, 51% yield). Mp = 172–176 °C (from acetone). ^{1}H NMR (400 MHz, DMSO-d_6) δ 10.39 (s, 1H, -CON*H*-), 8.53 (m, $J_{4,3}$ = 1.4 Hz, 1H, H-4), 8.16 (d, $J_{7,6}$ = 8.5 Hz, 1H, H-7), 7.94 (dd, $J_{6,7}$ = 8.5 Hz, $J_{6,4}$ = 1.4 Hz, 1H, H-6), 7.90 (d, $J_{3,2}$ = 5.5 Hz, 1H, H-3), 7.83 (s, 1H, H-2′), 7.74 (d, $J_{6',5'}$ = 8.3, Hz, 1H, H-6′), 7.62 - 7.57 (m, 2H, H-2, –SO_2N*H*-), 7.34 (m, 1H, H-5′), 7.09 (d, $J_{4',5'}$ = 7.5 Hz, 1H, H-5′), 4.17 (d, $J_{CH2,SO2NH}$ = 6.4 Hz, 1H, –CH_2-), 2.89 (s, 3H, -SO_2CH_3); ^{13}C NMR (100.6 MHz, DMSO-d_6) δ 165.7 (-*C*ONH-), 142.1 (C_{7a}), 139.4 ($C_{3'}$), 139.1 ($C_{1'}$), 138.8 (C_{3a}/C_5), 131.2 (C_{3a}/C_5), 129.0 (C_6), 128.6 ($C_{5'}$), 124.5 (C_7), 123.3 (C_3), 123.2 (C_4), 122.9 ($C_{4'}$), 122.6 (C_2), 119.6 ($C_{2'}$), 119.2 ($C_{6'}$), 46.1 (–CH_2–), 39.1 (-SO_2CH_3); IR (ATR) 3254, 1641, 1536, 1428, 1309, 1131 cm^{-1}. HRMS (ESI+) calcd. for [$C_{17}H_{16}N_2O_3S_2$+H]$^+$ [M+H]$^+$: 361.0681; found: 361.0668.

***tert*-Butyl (2-((3-(methylsulfonyl)phenyl)amino)-2-oxoethyl) carbamate, 13.** To the salt of 3-(methylsulfonyl)aniline hydrochloride, **11**, (1.01 g, 4.84 mmol) in dry THF (25 mL) under N_2 atmosphere, Et_3N (1.35 mL, 9.69 mmol) was added and the solution was stirred for 5 min at rt. Then, a solution of Boc-glycine, **12** (1.27 g, 7.26 mmol), HATU (2.21 g, 5.81 mmol), HOBt (785 mg, 8.81 mmol) and Et_3N (1.35 mL, 9.69 mmol) in dry THF/DMF (20 mL/3 mL) was added. The reaction mixture was stirred overnight at rt. The mixture was diluted with EtOAc (25 mL) and washed successively with water (3 x 30 mL), a saturated aqueous solution of $NaHCO_3$ (2 x 30 mL), and brine (3 x 30 mL). The solvent was evaporated under reduced pressure and the residue was diluted in methylene chloride (20 mL) washed again with water (3 x 60 mL) and brine (3 x 60 mL) in order to remove the remains of tetramethylurea. The organic layer was dried over anhydrous $MgSO_4$ and concentrated under vacuum to obtain the carbamate **13** as a brown solid (810 mg, 2.47 mmol, 51% yield). Mp = 100–104 °C (from acetone). ^{1}H NMR (250 MHz, $CDCl_3$) δ 8.81 (br s, 1H, -N*H*CO-), 8.03 (m, 1H, H-2′), 7.90 (d, $J_{4',6'}$ = 7.7 Hz, 1H, H-4′), 7.63 (d, $J_{6',5'}$ = 7.7 Hz, 1H, H-6′), 7.48 (m, 1H, H-5′), 5.45 (br s, 1H, -N*H*COO-), 3.97 (d, $J_{1,NHCOO}$ = 6.0 Hz, 2H, *H*-1), 3.06 (s, 3H, -SO_2CH_3), 1.47 (s, 9H, –C(CH_3)$_3$); ^{13}C NMR (100.6 MHz, $CDCl_3$) δ 168.6 (-NH*C*O-), 156.9 (-NH*C*OO-), 141.2 ($C_{3'}$), 138.9 ($C_{1'}$), 130.3 ($C_{5'}$), 125.0 ($C_{4'}$), 122.8 ($C_{6'}$), 118.4 ($C_{2'}$), 81.1 (-*C*(CH_3)$_3$), 45.6 (C_1), 44.5 (-SO_2CH_3), 1.47 (-C(*CH*$_3$)$_3$); IR (ATR) 3284, 2976, 1703, 1516, 1296, 1136 cm^{-1}. HRMS (ESI+) calcd. for [$C_{14}H_{20}N_2O_5S$+H]$^+$ [M+H]$^+$: 329.1171; found: 329.1157.

2-Amino-*N*-(3-(methylsulfonyl)phenyl)acetamide, 14. To a stirred solution of compound **13** (800 mg, 2.43 mmol) in CH_2Cl_2 (20 mL), trifluoroacetic acid (5 mL) was added. The mixture was stirred at rt until the starting material was consumed (TLC). Then, the mixture was concentrated under vacuum and the resulting brown syrup was taken up in acetone and precipitated with diethyl ether to deliver **14** (553 mg, 1.62 mmol, 66% yield) as a white solid. Mp = 179–183 °C (from acetone). ^{1}H NMR (400 MHz, DMSO-d_6) δ 11.01 (s, 1H, -CON*H*-), 8.29 (s, 3H, -NH_3^+), 8.24 (s, 1H, H-2′), 7.85 (br d, $J_{6'',5''}$ = 6.7 Hz, 1H, H-6′),

7.66 - 7.62 (m, 2H, H-4′, H-5′), 3.85 (s, 2H, H-1), 3.21 (s, 3H, -SO_2CH_3); ^{13}C NMR (100.6 MHz, DMSO-d_6) δ 165.5 (C_2), 158.5 (q, $J_{COCF3,F}$ = 31.3 Hz,$COCF_3^-$), 141.6 ($C_{3'}$), 139.0 ($C_{1'}$), 130.4 ($C_{4'}$), 123.7 ($C_{6'}$), 122.1 ($C_{5'}$), 117.8 (q, $J_{CF3,F}$ = 301 Hz, -CF_3), 117.0 ($C_{2'}$), 43.6 (C_1), 41.1 (-SO_2CH_3); IR (ATR) 3084, 1677, 1427, 1294, 1134 cm^{-1}. HRMS (ESI+) calcd. for [$C_{11}H_{13}F_3N_2O_5S$+H]$^+$ [M+H]$^+$: 229.0641; found: 229.0636.

***N*-(2-((3-(Methylsulfonyl)phenyl)amino)-2-oxoethyl)-*1H*-indole-5-carboxamide, 6a.** To a stirred solution of amine **14** (96 mg, 0.28 mmol) in dry THF (4 mL) under N_2 atmosphere, a solution of indole-5-carboxylic acid, **10a**, (68 mg, 0.42 mmol), EDCI (75 μL, 0.42 mmol), HOBt (57 mg, 0.42 mmol) and DIPEA (0.20 mL, 1.12 mmol) in dry THF/DMF (4 mL/1 mL) was added. The reaction mixture was stirred overnight at rt. Then, the reaction was quenched with water (10 mL) and extracted with EtOAc (10 mL). The organic layer was washed with water (3 x 10 mL), dried over anhydrous Na_2SO_4 and concentrated *in vacuo*. The residue was purified by recrystallization in Et_2O to furnish **6a** (81 mg, 0.22 mmol, 78% yield) as a white solid. Mp = > 230 °C (from acetone). ^{1}H NMR (400 MHz, DMSO-d_6) δ 11.34 (s, 1H, –NH–), 10.46 (s, 1H, -N*H*-2′), 8.71 (t, $J_{NHCO,1'}$ = 5.8 Hz, 1H, indole-CON*H*-), 8.28 (m, 1H, H-2″), 8.20 (m, 1H, H-4), 7.90 (m, 1H, H-6″), 7.68 (dd, $J_{6,7}$ = 8.6 Hz, $J_{6,4}$ = 1.8 Hz, 1H, H-6), 7.61 - 7.60 (m, 2H, H-4″, H-5″), 7.46 - 7.43 (m, 2H, H-2, H-7), 6.56 (m, 1H, H-3), 4.09 (d, $J_{1',NHCO}$ = 5.8 Hz, 2H, H-1′), 3.19 (s, 3H, -SO_2CH_3); ^{13}C NMR (100.6 MHz, DMSO-d_6): δ 168.9 ($C_{2'}$), 167.8 (indole-*C*ONH-), 141.3 ($C_{3''}$), 139.8 ($C_{1''}$), 137.5 (C_{7a}), 130.1 ($C_{5''}$), 127.0 (C_{3a}/C_5), 126.7 (C_2), 124.9 (C_{3a}/C_5), 123.6 ($C_{6''}$), 121.4 ($C_{4''}$), 120.6 (C_6), 120.2 (C_4), 117.0 ($C_{2''}$), 110.9 (C_7), 102.2 (C_3), 43.6 (-SO_2CH_3), 43.5 ($C_{1'}$); IR (ATR): 3395, 1705, 1617, 1427, 1292, 1139 cm^{-1}. HRMS (ESI+) calcd. for [$C_{19}H_{20}N_4O_4S$+H]$^+$ [M+H]$^+$: 372.1018; found: 372.1000.

***N*-(2-((3-(Methylsulfonyl)phenyl)amino)-2-oxoethyl)-2-naphthamide, 6b.** Compound **6b** was prepared as described for **6a** by using a solution of compound **14** (44 mg, 0.13 mmol) in dry THF (2 mL) and a solution of commercially available 2-naphtoic acid, **10b**, (35 mg, 0.19 mmol), EDCI (35 μL, 0.19 mmol), HOBt (26 mg, 0.19 mmol) and DIPEA (90 μL, 0.51 mmol) in dry THF/DMF (2 mL/1 mL). The residue was purified by recrystallization in Et_2O to furnish product **6b** as a white solid (48 mg, 0.13 mmol, 98% yield). Mp = 194–199 °C (from acetone). ^{1}H NMR (400 MHz, DMSO-d_6) δ 10.51 (s, 1H, -N*H*-2′), 9.08 (t, $J_{NHCO,1'}$ = 5.9 Hz, 1H, -N*H*CO-), 8.53 (s, 1H, H-1), 8.29 (m, 1H, H-2″), 8.06 - 7.98 (m, 4H, H-3/H-4/H-5/H-6/H-7/H-8), 7.91 (m, 1H, H-6″), 7.65 - 7.59 (m, 4H, H-5/H-6/H-7/H-8/H-4''/H-5″), 4.16 (d, $J_{1',NHCO}$ = 5.9 Hz, 2H, H-1′), 3.19 (s, 3H, -SO_2CH_3); ^{13}C NMR (100.6 MHz, DMSO-d_6) δ 168.5 (-NH*C*O-), 168.8 ($C_{2'}$), 141.3 ($C_{1''}$), 139.7 ($C_{3''}$), 134.2 (C_2), 132.1 (C_{4a}/C_{8a}), 131.2 (C_{4a}/C_{8a}), 130.1 ($C_{5''}$), 128.9/127.9/127.7/127.6/126.8/124.2 (C_1/C_3/C_4/C_5/C_6/C_7/C_8), 123.6 ($C_{6''}$), 121.5 ($C_{4''}$), 117.0 ($C_{2''}$), 43.6 (-SO_2CH_3), 43.5 ($C_{1'}$); IR (ATR) 3407, 3283, 1625, 1522, 1296, 1141 cm^{-1}. HRMS (ESI+) calcd. for [$C_{20}H_{18}N_2O_4S$+H]$^+$ [M+H]$^+$: 383.1066; found: 383.1048.

***N*-(3-(Methylsulfonyl)phenyl)-2-(2-(thiophen-3-yl)acetamido) acetamide, 6c.** Compound **6c** was prepared as described for **6a** by using a solution of compound **14** (91 mg, 0.27 mmol) in dry THF (4 mL) and a solution of commercially available 3-thiopheneacetic acid, **10c**, (57 mg, 0.40 mmol), EDCI (70 μL, 0.40 mmol), HOBt (54 mg, 0.40 mmol) and DIPEA (185 μL, 1.06 mmol) in dry THF/DMF (4 mL/1 mL). The residue was purified by recrystallization in Et_2O to furnish product **6c** as a white solid (70 mg, 0.20 mmol, 75% yield). Mp = 169–173 °C (from acetone). ^{1}H NMR (400 MHz, DMSO-d_6) δ 10.39 (s, 1H, -N*H*-1), 8.39 (t, $J_{NHCO,2}$ = 5.8 Hz, 1H, -N*H*CO-), 8.23 (m, 1H, H-2″), 7.85 (m, 1H, H-6″), 7.62 - 7.59 (m, 2H, H-4″,H-5″), 7.46 (m, 1H, H-5′), 7.29 (m, 1H, H-2′), 7.06 (m, 1H, H-4′), 3.92 (d, $J_{2,NHCO}$ = 5.8 Hz, 2H, H-2), 3.53 (s, 2H, -CH_2-thiophene), 3.19 (s, 3H, -SO_2CH_3); ^{13}C NMR (100.6 MHz, DMSO-d_6): δ 170.3 (-NH*C*O-), 168.4 (C_1), 141.3 ($C_{3''}$), 139.6 ($C_{1''}$), 135.9 ($C_{3'}$), 130.1 ($C_{5''}$), 128.8 ($C_{4'}$), 125.6 ($C_{5'}$), 123.5 ($C_{6''}$), 122.3 ($C_{2'}$), 121.5 ($C_{4''}$), 116.9 ($C_{2''}$), 43.6 (-SO_2CH_3), 42.8 (C_2), 36.7 (-CH_2-thiophene); IR (ATR) 3392, 3270, 1644, 1511, 1299, 1145 cm^{-1}. HRMS (ESI+) calcd. for [$C_{15}H_{16}N_2O_4S_2$+H]$^+$ [M+H]$^+$: 353.0630; found: 353.0615.

4-Ethyl-*N*-(2-((3-(methylsulfonyl)phenyl)amino)-2-oxoethyl) benzamide, 6d. Compound **6d** was prepared as described for **6a** by using a solution of compound **14** (90 mg, 0.26 mmol) in dry THF (4 mL) and a solution of commercially available 4-ethylbenzoic acid, **10d**, (59 mg, 0.39 mmol), EDCI (70 μL, 0.39 mmol), HOBt (53 mg, 0.39 mmol) and DIPEA (185 μL, 1.05 mmol) in dry THF/DMF (4 mL/1 mL). The residue was purified by recrystallization in Et_2O to furnish product **6d** as a white solid (84 mg, 0.23 mmol, 88% yield). Mp = 169–172 °C. ^{1}H NMR (400 MHz, DMSO-d_6) δ 10.46 (s, 1H, -N*H*-2′), 8.82 (t, $J_{NHCO,2'}$ = 5.8 Hz, 1H, -N*H*CO-), 8.26 (m, 1H, H-2″), 7.89 (m, 1H, H-6″), 7.84 (d, $J_{2,3}$ = $J_{6,5}$ = 8.3 Hz, 2H, H-2, H-6), 7.61 - 7.60 (m, 2H, H-4″,H-5″), 7.32 (d, $J_{2,3}$ = $J_{6,5}$ = 8.2 Hz, 2H, H-3, H,5), 4.08 (d, $J_{2',NHCO}$ = 5.8 Hz, 2H, H-2′), 3.19 (s, 3H, -SO_2CH_3), 2.67 (q, $J_{CH2,CH3}$ = 7.6 Hz, 2H, -CH_2CH_3), 1.20 (t, $J_{CH3,CH2}$ = 7.6 Hz, 2H, -CH_2CH_3); ^{13}C NMR (100.6 MHz, DMSO-d_6) δ 168.5 ($C_{2'}$), 166.6 (-NH*C*O-), 147.5 (C_4), 141.3 ($C_{3''}$), 139.7 ($C_{1''}$), 131.4 (C_1), 130.1 ($C_{5''}$), 127.7 (C_2, C_6), 127.4 (C_3, C_5), 123.6 ($C_{6''}$), 121.5 ($C_{4''}$), 117.0 ($C_{2''}$), 43.6 (-SO_2CH_3), 43.4 ($C_{1'}$), 28.0 (-CH_2CH_3), 15.3 (-CH_2CH_3); IR (ATR) 3422, 3274, 1705, 1638, 1303, 1147 cm^{-1}. HRMS (ESI+) calcd. for [$C_{18}H_{20}N_2O_4S$+H]$^+$ [M+H]$^+$: 361.1222; found: 361.1206.

***N*-(2-((3-(Methylsulfonyl)phenyl)amino)-2-oxoethyl)benzo [b] thiophene-3-carboxamide, 6e.** Compound **6e** was prepared as described for **6a** by using a solution of compound **14** (89 mg, 0.26 mmol) in dry THF (4 mL) and a solution of commercially available benzothiophene-3-carboxylic acid, **10e**, (70 mg, 0.39 mmol), EDCI (70 μL, 0.39 mmol), HOBt (53 mg, 0.39 mmol) and DIPEA (0.18 mL, 1.04 mmol) in dry THF/DMF (4 mL/1 mL). The residue was purified by recrystallization in Et_2O to furnish product **6e** as a white solid (96 mg, 0.25 mmol, 95% yield). Mp = 175–178 °C. ^{1}H NMR (400 MHz, DMSO-d_6) δ 10.52 (s, 1H, -N*H*-2′), 8.89 (t, $J_{NHCO,2'}$ = 5.8 Hz, 1H, -N*H*CO-), 8.49 (m, 1H, H-4), 8.46 (s, 1H, H-2), 8.29 (m, 1H, H-2″), 8.05 (m, 1H, H-7), 7.91 (m, 1H, H-6″), 7.63 - 7.61 (m, 2H, H-4″,H-5″), 7.48 - 7.41 (m, 2H, H-5, H-6), 4.13 (d, $J_{1',NHCO}$ = 5.8 Hz, 2H, H-1′), 3.20 (s, 3H, -SO_2CH_3); ^{13}C NMR (100.6 MHz, DMSO-d_6): δ 168.5 ($C_{2'}$), 163.6 (-NH*C*O-), 141.4 ($C_{3''}$), 139.7 ($C_{1''}$), 139.4 (C_{7a}), 131.3 (C_2), 130.4 (C_3), 130.1 ($C_{5''}$), 124.5 (C_5/C_6), 124.8 (C_5,/C_6), 123.6 ($C_{6''}$), 122.8 (C_7), 121.5 ($C_{4''}$), 117.0 ($C_{2''}$), 43.6 (-SO_2CH_3), 43.1 ($C_{1'}$); IR (ATR) 3328, 3084, 1623, 1530, 1322, 1146 cm^{-1}. HRMS (ESI+) calcd. for [$C_{18}H_{16}N_2O_4S_2$+H]$^+$ [M+H]$^+$: 411.0433; found: 411.0449.

***N*-(2-((3-(Methylsulfonyl)phenyl)amino)-2-oxoethyl)benzo [b] thiophene-5-carboxamide, 6f.** Compound **6f** was prepared as described for **6a** by using a solution of compound **14** (56 mg, 0.17 mmol) in dry THF (2 mL) and a solution of commercially available 1-benzothiophene-5-carboxylic acid, **10f**, (25 mg, 0.14 mmol), EDCI (24 μL, 0.15 mmol), HOBt (21 mg, 0.15 mmol) and DIPEA (100 μL, 0.56 mmol) in dry THF/DMF (2 mL/1 mL). The residue was purified by recrystallization in Et_2O to furnish product **6f** as a white solid (36 mg, 93 μmol, 66% yield). Mp = > 230 °C (from acetone). ^{1}H NMR (400 MHz, DMSO-d_6) δ 10.50 (s, 1H, -N*H*-2′), 8.99 (t, $J_{NHCO,1'}$ = 5.9 Hz, 1H, -N*H*CO-), 8.46 (m, 1H, H-4), 8.27 (m, 1H, H-2″), 8.12 (d, $J_{7,6}$ = 8.5 Hz,1H, H-7), 7.92 - 7.86 (m, 3H, H-3, H-6, H-6″), 7.63 - 7.57 (m, 3H, H-2, H-4″, H-5″), 4.12 (d, $J_{1',NHCO}$ = 5.9 Hz, 2H, H-1′), 3.19 (s, 3H, -SO_2CH_3); ^{13}C NMR (100.6 MHz, DMSO-d_6) δ 168.6 ($C_{2'}$), 166.9 (-NH*C*O-), 142.0 (C_{7a}), 141.4 ($C_{3''}$), 139.7 ($C_{1''}$), 139.2 (C_{3a}/C_5), 130.4 (C_{3a}/C_5), 130.2 ($C_{5''}$), 128.9 (C_6), 124.5 (C_2), 123.6 ($C_{6''}$), 123.0 (C_3, C_4), 122.5 (C_7), 121.6 ($C_{4''}$), 117.1 ($C_{2''}$), 43.6 (-SO_2CH_3), 43.5 ($C_{1'}$); IR (ATR) 3408, 3277, 1706, 1629, 1521, 1296, 1143 cm^{-1}. HRMS (ESI+) calcd. for [$C_{18}H_{16}N_2O_4S_2$+Na]$^+$ [M+Na]$^+$: 411.0449; found: 411.0437.

***tert*-Butyl *N*-[(3-nitrophenyl)sulfonyl] glycinate, 20.** To a solution of commercially available glycine *tert*-butyl ester HCl, **18** (3.08 g, 18.34 mmol) and 3-nitrobenzenesulfonyl chloride, **19**, (3.96 g, 17.86 mmol) in dry CH_2Cl_2 (110 mL), DIPEA (9.40 mL, 53.68 mmol) was added dropwise and the mixture was stirred for 2.5 h at rt. Then, the reaction was quenched with water (50 mL), the layers were separated, and the aqueous layer was extracted with CH_2Cl_2 (3 x 50 mL). The combined organic extracts were dried over anhydrous Na_2SO_4 and

concentrated under reduced pressure to deliver the sulphonamide **20** as a yellow solid (5.57 g, 17.61 mmol, 99% yield). Mp = 105–108 °C (from CH_2Cl_2). ^{1}H NMR (250 MHz, $CDCl_3$) δ 8.69 (m, 1H, H-2′), 8.42 (ddd, $J_{4',5'}$ = 8.2 Hz, $J_{4',6'}$ = 2.2 Hz, $J_{4',2'}$ = 1.1 Hz, 1H, H-4′), 8.20 (ddd, $J_{6',5'}$ = 8.2 Hz, $J_{6',4'}$ = 2.2 Hz, $J_{6',2'}$ = 1.1 Hz, 1H, H-6′), 7.74 (t, $J_{2',4'}$ = $J_{2',6'}$ = 8.2 Hz, 1H, H-2′), 5.48 (br t, 1H, –NHSO$_2$-), 3.77 (s, 2H, H-2), 1.34 (s, 9H, –C(CH_3)$_3$); ^{13}C NMR (100.6 MHz, $CDCl_3$) δ 167.8 (C_1), 148.2 ($C_{3'}$), 142.0 ($C_{1'}$), 132.9 ($C_{6'}$), 130.6 ($C_{5'}$), 127.2 ($C_{4'}$), 122.4 ($C_{2'}$), 83.2 (-*C*(CH$_3$)$_3$), 44.8 (C_2), 27.8 (-C(*C*H$_3$)$_3$); IR (ATR) 3164, 1738, 1523, 1441, 1349, 1236, 1162 cm^{-1}. HRMS (ESI+) calcd. for [$C_{12}H_{16}N_2O_6S$+Na]$^+$ [M+Na]$^+$: 339.0627; found: 339.0624.

***tert*-Butyl *N*-(*tert*-butoxycarbonyl)-*N*-[(3-nitrophenyl)sulfonyl] glycinate, 21.** To an ice-cooled solution of *tert*-butyl ester **20** (301 mg, 1.05 mmol) in anhydrous CH_3CN (5 mL), DMAP (52 mg, 0.42 mmol) and Boc_2O (546 mg, 2.48 mmol) were added. The solution was stirred at 0 °C for 30 min and then warmed up to rt and let to stir for 2 h. The solvent was removed under vacuum and the resulting residue was purified by column chromatography (hexane/EtOAc, from 4:1 to 3:1) to provide compound **21** (722 mg, 1.73 mmol, 82% yield) as a yellow solid. Mp = 80–84 °C (from CH_2Cl_2). ^{1}H NMR (360 MHz, $CDCl_3$) δ 8.88 (br t, $J_{2',4'}$ = $J_{2',6'}$ = 1.9 Hz, 1H, H-2′), 8.48 - 8.43 (m, 2H, H-4′, H-6′), 7.75 (t, $J_{5',4'}$ = $J_{5',6'}$ = 8.1 Hz, 1H, H-5′), 4.49 (s, 2H, H-1), 1.47 (s, 9H, –C(CH_3)$_3$), 1.35 (s, 9H, carbamate-C(CH_3)$_3$; ^{13}C NMR (90.5 MHz, $CDCl_3$) δ 167.5 (C_2), 150.1 (-NCOO*t*Bu), 147.9 ($C_{3'}$), 141.5 ($C_{1'}$), 134.7 ($C_{6'}$), 129.9 ($C_{5'}$), 128.0 ($C_{4'}$), 124.5 ($C_{2'}$), 85.8 (carbamate-*C*(CH$_3$)$_3$), 83.0 (-*C*(CH$_3$)$_3$), 47.8 (C_1), 28.1 (-C(*C*H$_3$)$_3$), 27.9 (carbamate-C(*C*H$_3$)$_3$); IR (ATR) 2981, 1730, 1533, 1360, 1346, 1145 cm^{-1}. HRMS (ESI+) calcd. for [$C_{17}H_{24}N_2O_8S$+Na]$^+$ [M+Na]$^+$: 439.1151; found: 439.1149.

***tert*-Butyl *N*-[(3-aminophenyl)sulfonyl]-*N*-(*tert*-butoxycarbonyl)glycinate, 22.** A mixture of **21** (1.57 g, 3.76 mmol) and 10% Pd/C (305 mg) in EtOAc (33 mL) was stirred under H_2 (1 atm) overnight. The suspension was filtered over Celite® and the filtrate was concentrated to obtain **22** as a white solid (1.45 g, 3.75 mmol, 99% yield). Mp = 109–111 °C (from CH_2Cl_2). ^{1}H NMR (360 MHz, acetone-d_6) δ 7.29 (m, 1H, H-2′), 7.27 - 7.21 (m, 2H, H-5′, H-6′), 6.95 (m, $J_{4',5'}$ = 7.6 Hz, 1H, H-4′), 5.18 (br s, 2H, –NH$_2$), 4.41 (s, 2H, H-1), 1.46 (s, 9H, –C(CH_3)$_3$), 1.35 (s, 9H, carbamate-C(CH_3)$_3$); ^{13}C NMR (90.5 MHz, acetone-d_6) δ 168.1 (C_2), 151.4 (-NCOO*t*Bu), 149.7 ($C_{3'}$), 141.7 ($C_{1'}$), 130.1 ($C_{5'}$), 119.5 ($C_{4'}$), 116.4 ($C_{6'}$), 114.0 ($C_{2'}$), 84.6 (carbamate-*C*(CH$_3$)$_3$), 82.3 (-*C*(CH$_3$)$_3$), 48.3 (C_1), 28.1 (-C(*C*H$_3$)$_3$), 28.0 (carbamate-C(*C*H$_3$)$_3$); IR (ATR) 3363, 2981, 1723, 1490, 1359, 1243, 1140 cm^{-1}. HRMS (ESI+) calcd. for [$C_{17}H_{26}N_2O_8S$+H]$^+$ [M+H]$^+$: 387.1590; found 387.1586.

***tert*-Butyl *N*-{[3-({*N*-[(benzyloxy)carbonyl]glycyl}amino)phenyl]sulfonyl}-*N*-(*tert*-butoxycarbonyl)glycinate, 24.** To a stirred solution of aniline **22** (84 mg, 0.22 mmol) in dry THF (2 mL) under N_2 atmosphere, a solution of Z-Gly-OH **23** (68 mg, 0.33 mmol), EDCI (60 μL, 0.34 mmol), HOBt (44 mg, 0.34 mmol) and Et_3N (0.12 mL, 0.86 mmol) in dry THF (2.5 mL) was added. The reaction mixture was stirred overnight at rt. The reaction was quenched with water (5 mL) and extracted with EtOAc (8 mL). Then, the organic layer was washed with water (3 x 10 mL) and brine (10 mL), dried over anhydrous Na_2SO_4 and concentrated. The residue was purified by column chromatography ($CHCl_3$/Et_2O, 2:1) to furnish a white solid identified as carbamate **24** (83 mg, 0.14 mmol, 66% yield). Mp = 134–137 °C (from CH_2Cl_2). ^{1}H NMR (360 MHz, acetone-d_6) δ 9.62 (s, 1H, –NH–2″), 8.35 (s, 1H, H-2′), 7.99 (br d, $J_{4',5'}$ = 8.8 Hz, 1H, H-4′), 7.77 (d, $J_{6',5'}$ = 7.9 Hz, 2H, H-6′), 7.42 - 7.23 (m, 5H, phenyl), 6.73 (t, $J_{NHCBz,1''}$ = 5.8 Hz, 1H, -N*H*CBz), 5.11 (s, 2H, -CH_2-phenyl), 4.45 (S, 2H, H-1), 4.02 (d, $J_{1'',NHCBz}$ = 6.0 Hz, 2H, H-1″), 1.46 (s, 9H, –C(CH_3)$_3$), 1.33 (s, 9H, carbamate-C(CH_3)$_3$); ^{13}C NMR (90.5 MHz, acetone-d_6) δ 169.2 ($C_{2''}$), 168.0 (C_2), 157.6 (-NH*C*Bz), 151.1 (-N*C*OO*t*Bu), 141.5 ($C_{1'}$), 140.1 ($C_{3'}$), 138.0 ($C_{1'''}$), 130.1 ($C_{5'}$), 129.2 ($C_{4'''}$), 128.7 ($C_{2'''}$, $C_{3'''}$), 124.7 ($C_{4'}$), 123.7 ($C_{6'}$), 119.7 ($C_{2'}$), 85.0 (carbamate-*C*(CH$_3$)$_3$), 82.5 (-*C*(CH$_3$)$_3$), 66.9 (-*C*H$_2$-phenyl), 48.5 (C_1), 45.6 ($C_{1''}$), 28.1 (-C(*C*H$_3$)$_3$), 27.9 (carbamate-C(*C*H$_3$)$_3$); IR (ATR) 3423, 3288, 1687, 1509, 1348, 1232, 1143 cm^{-1}. HRMS (ESI+) calcd. for [$C_{27}H_{35}N_3O_9S$+Na]$^+$ [M+Na]$^+$: 600.1992; found: 600.1985.

***tert*-Butyl *N*-(*tert*-butoxycarbonyl)-*N*-{[3-(glycylamino)phenyl]sulfonyl}glycinate, 25.** A mixture of **24** (262 mg, 0.45 mmol) and 10% Pd/C (33 mg) in MeOH (7.3 mL) was stirred under H_2 (1 atm) overnight. The suspension was filtered over Celite® and the filtrate was concentrated to obtain **25** as a brown solid (199 mg, 0.45 mmol, quant.). Mp = 81–83 °C (from CH_2Cl_2). ^{1}H NMR (360 MHz, $CDCl_3$) δ 9.67 (s, 1H, –NHCO–), 8.18 (dd, $J_{4',5'}$ = 8.0 Hz, $J_{4',2'}$ = 1.9 Hz, 1H, H-4′), 8.01 (t, $J_{2',4'}$ = $J_{2',6'}$ = 1.9 Hz, 1H, H-2′), 7.77 (ddd, $J_{6',5'}$ = 8.1 Hz, $J_{6',2'}$ = 1.9 Hz, $J_{6',4'}$ = 0.9 Hz, 2H, H-6′), 7.47 (t, $J_{5',4'}$ = $J_{5',6'}$ = 8.0 Hz 1H, H-5′), 4.45 (s, 2H, H-1), 3.48 (d, $J_{1'',NH2}$ = 3.3 Hz, 2H, H-1″), 1.67 (br s, 2H, –NH$_2$), 1.46 (s, 9H, –C(CH_3)$_3$), 1.33 (s, 9H, carbamate-C(CH_3)$_3$); ^{13}C NMR (90.5 MHz, $CDCl_3$): δ 171.1 ($C_{2''}$), 167.5 (C_2), 150.5 (-N*C*OO*t*Bu), 140.5 ($C_{1'}$/$C_{3'}$), 138.2 ($C_{1'}$/$C_{3'}$), 129.6 ($C_{5'}$), 124.2 ($C_{4'}$), 123.7 ($C_{6'}$), 119.0 ($C_{2'}$), 85.0 (carbamate-*C*(CH$_3$)$_3$), 82.5 (-*C*(CH$_3$)$_3$), 47.7 (C_1), 45.2 ($C_{1''}$), 28.1 (-C(*C*H$_3$)$_3$), 28.0 (carbamate-C(*C*H$_3$)$_3$); IR (ATR): 2981, 1731, 1478, 1356, 1249, 1139 cm^{-1}. HRMS (ESI+) calcd. for [$C_{19}H_{29}N_3O_7S$+H]$^+$ [M+H]$^+$: 444.1804; found: 444.1804.

***tert*-Butyl *N*-(*tert*-butoxycarbonyl)-*N*-[(3-{[*N*-(3-thienylacetyl)glycyl]amino}phenyl)sulfonyl] glycinate, 26c.** To a stirred solution of aniline **25** (153 mg, 0.35 mmol) in dry THF (4 mL) under N_2 atmosphere, a solution of 3-thiopheneacetic acid, **10c**, (68 mg, 0.46 mmol), EDCI (80 μL, 0.46 mmol), HOBt (58 mg, 0.43 mmol) and DIPEA (0.20 mL, 1.15 mmol) in dry THF (4 mL) was added. The reaction mixture was stirred overnight at rt. Then, the mixture was quenched with water (5 mL) and extracted with EtOAc (8 mL). The organic layer was washed with water (3 x 10 mL) and brine (10 mL). The organic layer was dried over anhydrous Na_2SO_4 and concentrated *in vacuo*. The residue was purified by recrystallization in hexane/EtOAc (2:1) to furnish **26c** as a white solid (105 mg, 0.18 mmol, 65% yield). Mp = 130–134 °C (from CH_2Cl_2). ^{1}H NMR (360 MHz, acetone-d_6) δ 9.57 (s, 1H, –NH–1″), 8.32 (br t, 1H, H-2′), 7.93 (br d, $J_{4',5'}$ = 8.0 Hz, 1H, H-4′), 7.76 (d, $J_{6',5'}$ = 8.0 Hz, 1H, H-6′), 7.57 (t, $J_{5',4'}$ = $J_{5',6'}$ = 8.0 Hz, 1H, H-5′), 7.52 (m, 1H, –NHCO–), 7.41 (br dd, $J_{5''',4'''}$ = 4.7 Hz, $J_{5''',2'''}$ = 3.0 Hz, 1H, H-5‴), 7.31 (br s, 1H, H-2‴), 7.12 (d, $J_{4''',5'''}$ = 4.7 Hz, 1H, H-4‴), 4.46 (s, 2H, H-2), 4.07 (s, 2H, H-2″), 3.65 (s, 2H, -CH_2-thiophene), 1.46 (s, 9H, –C(CH_3)$_3$), 1.34 (s, 9H, carbamate-C(CH_3)$_3$); ^{13}C NMR (100.6 MHz, acetone-d_6) δ 171.5 (-NH*C*O-), 168.9 ($C_{1''}$), 168.1 (C_1), 151.2 (-N*C*OO*t*Bu), 141.6 ($C_{1'}$), 140.1 ($C_{3'}$), 136.6 ($C_{1'''}$), 130.2 ($C_{5'}$), 129.6 ($C_{4'''}$), 126.4 ($C_{5'''}$), 124.7 ($C_{4'}$), 123.8 ($C_{6'}$), 123.4 ($C_{2'''}$), 119.7 ($C_{2'}$), 85.1 (carbamate-*C*(CH$_3$)$_3$), 82.5 (-*C*(CH$_3$)$_3$), 48.5 (C_1), 44.3 ($C_{1''}$), 38.0 (-*C*H$_2$-thiophene), 28.1 (-C(*C*H$_3$)$_3$), 28.0 (carbamate-C(*C*H$_3$)$_3$); IR (ATR) 3391, 3274, 2975, 1740, 1640, 1360, 1300, 1146 cm^{-1}. HRMS (ESI+) calcd. for [$C_{25}H_{33}N_3O_8S_2$+Na]$^+$ [M+H]$^+$: 590.1607; found: 590.1603.

***tert*-Butyl *N*-(*tert*-butoxycarbonyl)-*N*-[(3-{[*N*-(4-ethylbenzoyl)glycyl]amino}phenyl)sulfonyl] glycinate, 26d.** Compound **26d** was prepared as described for **26c** by using solution of compound **25** (202 mg, 0.46 mmol) in dry THF (5 mL) and a solution of a solution of 4-ethylbenzoic acid, **10d** (109 mg, 0.73 mmol), EDCI (120 μL, 0.73 mmol), HOBt (101 mg, 0.68 mmol) and DIPEA (0.32 mL, 1.84 mmol) in dry THF (6 mL) was added. The residue was purified by flash column chromatography (hexane/EtOAc, from 2:1 to 1:1) to furnish a white solid identified as compound **26d** (227 mg, 0.39 mmol, 87% yield). Mp = 78–81 °C (from CH_2Cl_2). ^{1}H NMR (360 MHz, acetone-d_6) δ 9.71 (s, 1H, –NH–2″), 8.34 (br t, $J_{2',4'}$ = $J_{2',6'}$ = 1.9 Hz, 1H, H-2′), 8.11 (br t, $J_{NHCO,1''}$ = 5.8 Hz, 1H, -N*H*CO-), 8.01 (dd, $J_{4',5'}$ = 8.2 Hz, $J_{4',2'}$ = 1.9 Hz, 1H, H-4′), 7.89 (d, $J_{2''',3'''}$ = 8.1 Hz, 2H, H-2‴), 7.76 (dd, $J_{6',5'}$ = 8.0 Hz, $J_{6',2'}$ = 1.7 Hz, 1H, H-6′), 7.56 (t, $J_{5',4'}$ = $J_{5',6'}$ = 8.1 Hz, 1H, H-5′), 7.33 (d, $J_{3''',2'''}$ = 8.1 Hz, 2H, H-3‴), 4.44 (s, 2H, H-1), 4.24 (d, $J_{1'',NHCO}$ = 5.8 Hz 2H, H-1″), 2.70 (q, $J_{CH2CH3,CH3}$ = 7.7 Hz, 2H, -CH_2CH$_3$), 1.45 (s, 9H, –C(CH_3)$_3$), 1.33 (s, 9H, carbamate-C(CH_3)$_3$), 1.23 (t, $J_{CH3,CH2CH3}$ = 7.7 Hz, 2H, -CH$_2$CH_3); ^{13}C NMR (90.5 MHz, acetone-d_6) δ 169.2 ($C_{2''}$), 168.0 (C_2), 167.9 (-NH*C*O-), 151.2 (-N*C*OO*t*Bu), 148.9 ($C_{4'''}$), 141.5 ($C_{1'}$/$C_{3'}$), 140.2 ($C_{1'}$/$C_{3'}$), 132.6 ($C_{1'''}$), 130.1 ($C_{5'}$), 128.7 ($C_{3'''}$), 128.3 ($C_{2'''}$), 124.8 ($C_{4'}$), 123.7 ($C_{6'}$), 119.8 ($C_{2'}$), 85.0 (carbamate-*C*(CH$_3$)$_3$), 82.5 (-*C*(CH$_3$)$_3$), 48.5 (C_1), 44.8 ($C_{1''}$), 29.3 (-*C*H$_2$CH$_3$), 28.1 (-C(*C*H$_3$)$_3$), 28.0 (carbamate-C(*C*H$_3$)$_3$), 15.8 (-CH$_2$*C*H$_3$); IR (ATR) 3280, 2923, 1731,

1536, 1479, 1360, 1141 cm^{-1}. HRMS (ESI+) calcd. for $[C_{28}H_{37}N_3O_8S+Na]^+$ $[M+Na]^+$: 598.2199; found: 598.2204.

***tert*-Butyl *N*-[(3-{[*N*-(1-benzothien-3-ylcarbonyl)glycyl] amino} phenyl)sulfonyl] -*N*-(*tert*-butoxycarbonyl)glycinate, 26e.** Compound **26e** was prepared as described for **26c** by using a solution of compound **25** (153 mg, 0.35 mmol) in dry THF (6 mL) and a solution of commercially available benzothiophene-3-carboxylic acid, **10e** (94 mg, 0.53 mmol), EDCI (90 μL, 0.51 mmol), HOBt (73 mg, 0.54 mmol) and DIPEA (0.24 mL, 1.38 mmol) in dry THF (6 mL). The residue was purified by column chromatography ($CHCl_3/Et_2O$, 2:1) to furnish **26e** as a white solid (198 mg, 0.33 mmol, 95% yield). Mp = 134–137 °C (from CH_2Cl_2). ^{1}H NMR (400 MHz, DMSO-d_6) δ 10.50 (s, 1H, -N*H*-1″), 8.87 (t, $J_{NHCO,2''}$ = 6.0 Hz, 1H, -N*H*CO-), 8.48 (m, 1H, H-4‴), 8.45 (s, 1H, H-2‴), 8.32 (br t, $J_{2',4'} = J_{2',6'}$ = 1.9 Hz, 1H, H-2′), 8.06 (m, 2H, H-7‴), 7.92 (br ddd, $J_{4',5'}$ = 8.1 Hz, $J_{4',2'}$ = 1.9 Hz, $J_{4',6'}$ = 1.1 Hz, 1H, H-4′), 7.68 (br ddd, $J_{6',5'}$ = 7.9 Hz, $J_{6',2'}$ = 1.8 Hz, $J_{6',4'}$ = 1.1 Hz, 1H, H-6′), 7.60 (t, $J_{5',4'} = J_{5',6'}$ = 8.0 Hz, 1H, H-5′), 7.47 - 7.41 (m, 2H, H-5‴, H-6‴), 4.41 (s, 2H, H-2), 4.12 (d, $J_{2'',NHCO}$ = 6.0 Hz, 2H, H-2″), 1.40 (s, 9H, –C(CH_3)$_3$), 1.27 (s, 9H, carbamate-C(CH_3)$_3$; ^{13}C NMR (100.6 MHz, DMSO-d_6) δ 168.5 ($C_{1''}$), 167.0 (C_1), 163.6 (-NH*C*O-), 149.9 (-N*C*OO*t*Bu), 139.7 ($C_{1'}$), 139.4 ($C_{3'}$), 139.3 ($C_{3a'''}$), 137.2 ($C_{7a'''}$), 131.3 ($C_{2''}$), 130.4 ($C_{3''}$), 129.7 ($C_{5'}$), 124.9 ($C_{6''}$), 124.8 ($C_{5''}$), 124.5 ($C_{4''}$), 123.8 ($C_{4'}$), 122.7 ($C_{7''}$), 122.1 ($C_{6'}$), 118.3 ($C_{2'}$), 84.3 (carbamate-*C*(CH$_3$)$_3$), 81.8 (-*C*(CH$_3$)$_3$), 47.7 (C_2), 43.0 ($C_{2''}$), 27.5 (-C(*C*H$_3$)$_3$), 27.3 (carbamate-C(*C*H$_3$)$_3$); IR (ATR) 3260, 2981, 1733, 1628, 1348, 1228, 1138, cm^{-1}. HRMS (ESI+) calcd. for $[C_{28}H_{33}N_3O_8S_2+H]^+$ $[M+H]^+$: 604.1787; found: 604.1771.

***tert*-Butyl *N*-(*tert*-butoxycarbonyl)-*N*-{[3-({*N*-[4-(methylamino) benzoyl] glycyl}amino) phenyl] sulfonyl}glycinate, 26h.** Compound **26h** was prepared as described for **26c** by using a solution of compound **25** (128 mg, 0.29 mmol) in dry THF (5 mL) and a solution of commercially available 4-(methylamino)benzoic acid, **10h** (70 mg, 0.46 mmol), EDCI (80 μL, 0.45 mmol), HOBt (60 mg, 0.44 mmol) and DIPEA (0.20 mL, 1.15 mmol) in dry THF (5 mL). The residue was purified by column chromatography (hexane/EtOAc, 1:1) to furnish **26h** as a white solid (155 mg, 0.27 mmol, 93% yield). Mp = 100–103 °C (from CH_2Cl_2). ^{1}H NMR (400 MHz, acetone-d_6) δ 9.78 (s, 1H, –NH–1″), 8.34 (s, 1H, H-2′), 7.99 (d, $J_{4',5'}$ = 8.1 Hz, 1H, H-4′), 7.87 (br s, 1H, -N*H*CO-), 7.79 (d, $J_{2'',3''}$ = 8.5 Hz, 2H, H-2‴), 7.74 (d, $J_{6',5'}$ = 8.1 Hz, 1H, H-6′), 7.54 (t, $J_{5',4'} = J_{5',6'}$ = 8.1 Hz, 1H, H-5′), 6.62 (d, $J_{3'',2''}$ = 8.4 Hz, 2H, H-3‴), 5.57 (br q, $J_{NHCH3,CH3}$ = 5.2 Hz, 1H, -N*H*CH$_3$), 4.44 (s, 2H, H-2), 4.21 (d, $J_{2'',NHCO}$ = 5.2 Hz 2H, H-2″), 2.83 (d, $J_{CH3,NHCH3}$ = 5.2 Hz, 3H, -C*H*$_3$), 1.47 (s, 9H, –C(CH_3)$_3$), 1.33 (s, 9H, carbamate-C(CH_3)$_3$); ^{13}C NMR (100.6 MHz, acetone-d_6) δ 169.7 ($C_{1''}$), 168.2 (-NH*C*O-), 168.0 (C_1), 153.7 ($C_{4''}$), 151.2 (-N*C*OO*t*Bu), 141.5 ($C_{1'}$), 140.3 ($C_{3'}$), 130.1 ($C_{5'}$), 129.8 ($C_{2''}$), 124.8 ($C_{4'}$), 123.7 ($C_{6'}$), 121.8 ($C_{1''}$), 119.7 ($C_{2'}$), 111.6 ($C_{3''}$), 85.0 (carbamate-*C*(CH$_3$)$_3$), 82.5 (-*C*(CH$_3$)$_3$), 48.5 (C_1), 45.0 ($C_{1''}$), 29.6 (-*C*H$_3$), 28.1 (-C(*C*H$_3$)$_3$), 28.0 (carbamate-C(*C*H$_3$)$_3$); IR (ATR) 3414, 2980, 1730, 1604, 1509, 1302, 1140 cm^{-1}. HRMS (ESI+) calcd. for $[C_{27}H_{36}N_4O_8S+H]^+$ $[M+H]^+$: 577.2332; found: 577.2329.

***tert*-Butyl *N*-(*tert*-butoxycarbonyl)-*N*-[(3-{[*N*-(quinolin-3-ylcarbonyl)glycyl] amino}phenyl) sulfonyl] glycinate, 26i.** Compound **26i** was prepared as described for **26c** by using a solution of compound **25** (36 mg, 81 μmol) in dry THF (1.5 mL) and a solution of commercially available 3-quinolinecarboxylic acid, **10i**, (27 mg, 0.16 mmol), EDCI (22 μL, 0.13 mmol), HOBt (20 mg, 0.15 mmol) and DIPEA (60 μL, 0.34 mmol) in dry THF/DMF (2 mL/0.2 mL). The residue was purified by column chromatography (EtOAc, 100%) to furnish **26i** as a yellow solid (42 mg, 0.07 mmol, 86% yield). Mp = 155 °C (from CH_2Cl_2). ^{1}H NMR (360 MHz, acetone-d_6) δ 9.77 (s, 1H, –NH–1″), 9.40 (d, $J_{2'',4''}$ = 2.0 Hz, 1H, H-2‴), 8.87 (d, $J_{4'',2''}$ = 2.0 Hz, 1H, H-4‴), 8.54 (br t, $J_{NHCO,2''}$ = 5.6 Hz, 1H, -N*H*CO-), 8.37 (s, 1H, H-2′), 8.11 (d, $J_{8'',7''}$ = 8.7 Hz, 1H, H-8‴), 8.07 (d, $J_{5'',6''}$ = 8.0 Hz, 1H, H-5‴), 8.01 (d, $J_{4',5'}$ = 8.2 Hz, 1H, H-4′), 7.87 (m, 1H, H-7‴), 7.77 (d, $J_{6',5'}$ = 8.1 Hz, 1H, H-6′), 7.68 (m, 1H, H-6‴), 7.57 (t, $J_{5',4'} = J_{5',6'}$ = 8.1 Hz, 1H, H-5′), 4.45 (s, 2H, H-2), 4.36 (d, $J_{2'',NHCO}$ = 5.8 Hz, 2H, H-2″), 1.45 (s, 9H, –C(CH_3)$_3$), 1.33 (s, 9H, carbamate-C(CH_3)$_3$); ^{13}C NMR (90.5 MHz, acetone-d_6): δ 168.8 ($C_{1''}$), 168.0 (C_1), 166.6 (-NH*C*O-), 151.2 (-N*C*OO*t*Bu), 150.2 ($C_{8a'''}$), 149.8 ($C_{2''}$), 141.5 ($C_{1'}$), 140.1 ($C_{3'}$), 136.3 ($C_{4''}$), 131.9 ($C_{7''}$), 130.2 ($C_{8''}$), 130.1 ($C_{5'}$), 129.9 ($C_{5''}$), 128.2 ($C_{6''}$), 127.7 ($C_{3''}$), 127.6 ($C_{4a'''}$), 124.8 ($C_{4'}$), 123.8 ($C_{6'}$), 119.8 ($C_{2'}$), 85.0 (carbamate-*C*(CH$_3$)$_3$), 82.5 (-*C*(CH$_3$)$_3$), 48.5 (C_1), 44.7 ($C_{1''}$), 28.1 (-C(*C*H$_3$)$_3$), 28.0 (carbamate-C(*C*H$_3$)$_3$); IR (ATR) 3281, 2980, 1730, 1647, 1535, 1358, 1140 cm^{-1}. HRMS (ESI+) calcd. for $[C_{29}H_{34}N_4O_8S+H]^+$ $[M+H]^+$: 599.2176; found 599.2168.

***N*-[(3-{[*N*-(3-Thienylacetyl)glycyl] amino}phenyl)sulfonyl] glycine, 17c.** To a stirred solution of compound **28c** (104 mg, 0.18 mmol) in CH_2Cl_2 (1.0 mL), trifluoroacetic acid (0.77 mL, 10.07 mmol) was added. The mixture was stirred at rt for 5 h. Then, the solution was concentrated under vacuum and the resulting solid was washed with cold CH_2Cl_2 to furnish **17c** as a white solid (74 mg, 0.18 mmol, quant. yield). Mp = 175–179 °C (from CH_2Cl_2). ^{1}H NMR (400 MHz, DMSO-d_6) δ 12.68 (br s, 1H, –COOH), 10.32 (s, 1H, –NH–2″), 8.39 (t, $J_{NHCO,1''}$ = 5.8 Hz, 1H, –NHCO–), 8.11 (s, 1H, H-2′), 8.06 (m, 1H, –NHSO$_2$-), 7.79 (d, $J_{4',5'}$ = 7.9 Hz, 1H, H-4′), 7.51 (t, $J_{5',4'} = J_{5',6'}$ = 7.8 Hz, 1H, H-5′), 7.47 - 7.45 (m, 2H, H-6′, H-5‴), 7.29 (m, 1H, H-2‴), 7.07 (dd, $J_{4''',5'''}$ = 4.9 Hz, $J_{4''',2'''}$ = 1.1 Hz, 1H, H-4‴), 3.92 (m, 2H, H-1″), 3.58 (d, $J_{1,NHSOO}$ = 5.7 Hz, 2H, H-1), 3.54 (s, 2H, –CH$_2$-thiophene); ^{13}C NMR (100.6 MHz, DMSO-d_6): δ 170.4 (C_2), 170.2 (–NHCO–), 168.3 ($C_{2''}$), 141.2 ($C_{1'}$), 139.4 ($C_{3'}$), 136.0 ($C_{3''}$), 129.7 ($C_{5'}$), 128.8 ($C_{4''}$), 125.7 ($C_{5''}$), 122.5 ($C_{4'}$), 122.3 ($C_{2''}$), 121.0 ($C_{6'}$), 116.8 ($C_{2'}$), 43.8 (C_1), 42.8 ($C_{1''}$), 36.8 (–CH$_2$–thiophene); IR (ATR) 3265, 2402, 1728, 1627, 1413, 1341, 1247, 1159 cm^{-1}. HRMS (ESI-) calcd. for $[C_{16}H_{17}N_3O_6S_2–H]^-$ $[M-H]^-$: 410.0481; found: 410.0488.

***N*-[(3-{[*N*-(4-Ethylbenzoyl)glycyl] amino}phenyl)sulfonyl] glycine, 17d.** Compound **17d** was prepared as described for **17c** by using compound **26d** (208 mg, 0.36 mmol), TFA (1.50 mL, 19.87 mmol) in CH_2Cl_2 (2.20 mL). The residue was washed with CH_2Cl_2 to furnish **17d** as a white solid (150 mg, 0.36 mmol, quant.). Mp = 222–225 °C (from CH_2Cl_2). ^{1}H NMR (400 MHz, DMSO-d_6) δ 10.38 (s, 1H, -N*H*-2″), 8.80 (t, $J_{NHCO,1''}$ = 5.9 Hz, 1H, -N*H*CO-), 8.13 (br t, $J_{2',4'} = J_{2',6'}$ = 1.8 Hz, 1H, H-2′), 8.07 (br t, $J_{NHSOO,1}$ = 5.9 Hz, 1H, -N*H*SO$_2$-), 7.84 (d, $J_{2''',3'''}$ = 8.3 Hz, 2H, H-2‴), 7.81 (m, 3H, H-4′), 7.51 (t, $J_{5',4'} = J_{5',6'}$ = 7.9 Hz, 1H, H-5′), 7.47 (dt, $J_{6',5'}$ = 8.0 Hz, $J_{6',2'} = J_{6',4'}$ = 1.5 Hz, 1H, H-6′), 7.32 (d, $J_{3''',2'''}$ = 8.3 Hz, 2H, H-3‴), 4.07 (d, $J_{1'',NHCO}$ = 5.9 Hz, 2H, H-1″), 3.58 (d, $J_{1,NHSOO}$ = 5.7 Hz 2H, H-1), 2.66 (q, $J_{CH2CH3,CH3}$ = 7.4 Hz, 2H, -C*H*$_2$CH$_3$), 1.20 (t, $J_{CH3,CH2CH3}$ = 7.5 Hz, 2H, -C*H*$_3$); ^{13}C NMR (100.6 MHz, DMSO-d_6): δ 170.2 (C_2), 168.4 ($C_{2''}$), 166.6 (-NH*C*O-), 147.5 ($C_{4''}$), 141.2 ($C_{1'}$/$C_{3'}$), 139.5 ($C_{1'}$/$C_{3'}$), 131.4 ($C_{1''}$), 129.7 ($C_{5'}$), 127.7 ($C_{3''}$), 127.5 ($C_{2''}$), 122.5 ($C_{4'}$), 121.0 ($C_{6'}$), 116.9 ($C_{2'}$), 43.8 (C_1), 43.4 ($C_{1''}$), 28.1 (-*C*H$_2$CH$_3$), 15.8 (-CH$_2$*C*H$_3$); IR (ATR) 3324, 2935, 1731, 1598, 1544, 1306, 1149 cm^{-1}. HRMS (ESI+) calcd. For $[C_{19}H_{21}N_3O_6S+H]^+$ $[M+H]^+$: 420.1229; found: 420.1216.

***N*-[(3-{[*N*-(1-Benzothien-3-ylcarbonyl)glycyl] amino}phenyl) sulfonyl] glycine, 17e.** Compound **17e** was prepared as described for **17c** by using compound **26e** (114 mg, 0.19 mmol), TFA (0.79 mL, 10.32 mmol) in CH_2Cl_2 (2.2 mL). The residue was washed with hexane/Et_2O (1:1) to furnish **17e** as a white solid (84 mg, 0.19 mmol, quant.). Mp = 213–216 °C (from CH_2Cl_2). ^{1}H NMR (400 MHz, DMSO-d_6) δ 10.44 (s, 1H, -N*H*-1″), 8.87 (t, $J_{NHCO,2''}$ = 5.9 Hz, 1H, -N*H*CO-), 8.48 (m, 1H, H-4‴), 8.46 (s, 1H, H-2‴), 8.14 (br t, $J_{2',4'} = J_{2',6'}$ = 1.8 Hz, 1H, H-2′), 8.09 (t, $J_{NHSOO,2}$ = 6.2 Hz, 1H, -N*H*SO$_2$-), 8.06 (m, 1H, H-7‴), 7.84 (m, 1H, H-4′), 7.53 (t, $J_{5',4'} = J_{5',6'}$ = 7.9 Hz, 1H, H-5′), 7.49 (m, 1H, H-6′), 7.47 - 7.40 (m, 2H, H-5‴, H-6‴), 4.12 (d, $J_{2'',NHCO}$ = 5.9 Hz, 2H, H-2″), 3.58 (d, $J_{2,NHSOO}$ = 6.2 Hz, 2H, H-2); ^{13}C NMR (100.6 MHz, DMSO-d_6) δ 170.2 (C_1), 168.4 ($C_{1''}$), 163.6 (-NH*C*O-), 141.2 ($C_{1'}$), 139.5 ($C_{3'}$), 139.5 ($C_{3a'''}$), 137.2 ($C_{7a'''}$), 131.3 ($C_{2''}$), 130.4 ($C_{3''}$), 129.7 ($C_{5'}$), 124.9 ($C_{6''}$), 124.9 ($C_{5''}$), 124.5 ($C_{4''}$), 122.8 ($C_{7''}$), 122.5 ($C_{4'}$), 121.1 ($C_{6'}$), 116.9 ($C_{2'}$), 43.8 (C_2), 43.0 ($C_{2''}$); IR (ATR) 3256, 1732, 1633, 1531, 1408, 1306, 1159 cm^{-1}. HRMS (ESI+): calcd. for $[C_{19}H_{17}N_3O_6S_2+H]^+$ $[M+H]^+$: 448.0637; found: 448.0633.

***N*-{[3-({*N*-[(Benzyloxy)carbonyl] glycyl}amino)phenyl]**

sulfonyl}glycine, 17g. To a stirred solution of compound **24** (231 mg, 0.40 mmol) in CH_2Cl_2 (2.0 mL), TFA (1.69 mL, 22.08 mmol) was added. The mixture was stirred at rt for 5 h. Then, the solution was concentrated under vacuum and the resulting solid was washed with hexane/Et_2O (1:1) to furnish **17g** as a white solid (166 mg, 0.39 mmol, quant. yield). Mp = 160–165 °C (from CH_2Cl_2). ^{1}H NMR (360 MHz, DMSO-d_6) δ 12.70 (br s, 1H, -COO*H*), 10.31 (s, 1H, -N*H*-2″), 8.10 (s, 1H, H-2′), 8.08 (t, $J_{NHSO2,1}$ = 5.8 Hz, 1H, –NHSO$_2$-), 7.80 (d, $J_{4',5'}$ = 7.9 Hz, 1H, H-4′), 7.61 (br t, $J_{NHCOO,1''}$ = 5.9 Hz, 1H, -N*H*CBz), 7.53 - 7.45 (m, 2H, H-5′, H-6′), 7.38 - 7.23 (m, 5H, phenyl), 5.05 (s, 2H, -C*H*$_2$-phenyl), 3.82 (d, $J_{1'',NHCOO}$ = 6.2 Hz, 2H, H-1″), 3.56 (s, d, $J_{1,NHSOO}$ = 6.1 Hz, 2H, H-1″); ^{13}C NMR (90.5 MHz, DMSO-d_6) δ 170.2 (C$_2$), 168.5 (C$_{2''}$), 156.6 (-NH*C*Bz), 141.2 (C$_{1'}$), 139.4 (C$_{3'}$), 137.0 (C$_{1'''}$), 129.7 (C$_{5'}$), 128.4 (C$_{3''}$), 127.8 (C$_{2'''}$, C$_{4'''}$), 122.4 (C$_{4'}$), 121.0 (C$_{6'}$), 116.8 (C$_{2'}$), 65.6 (-*C*H$_2$-phenyl), 44.1 (C$_{1''}$), 43.8 (C$_1$). IR (ATR): 3285, 1685, 1594, 1525, 1433, 1246, 1154 cm^{-1}. HRMS (ESI+): calcd. for [$C_{18}H_{19}N_3O_7S$+Na]$^+$: 444.0841; [M+Na]$^+$ found: 444.0839.

***N*-{[3-({*N*-[4-(Methylamino)benzoyl]glycyl}amino)phenyl] sulfonyl}glycine, 17h.** Compound **17h** was prepared as described for **17c** by using compound **26h** (84 mg, 0.15 mmol), TFA (0.61 mL, 8.03 mmol) in CH_2Cl_2 (0.8 mL). The residue was solved in acetone and CH_2Cl_2 was added to precipitate **17h** as a white solid (60 mg, 0.14 mmol, quant). Mp = 225–230 °C (from CH_2Cl_2). ^{1}H NMR (400 MHz, DMSO-d_6) δ 10.33 (s, 1H, –NH–1″), 8.43 (br t, $J_{NHCO,2''}$ = 5.5 Hz, 1H, -N*H*CO-), 8.12 (s, 1H, H-2′), 8.07 (t, $J_{NHSOO,2}$ = 5.9 Hz, 1H, –NHSO$_2$-), 7.82 (d, $J_{4',5'}$ = 8.0 Hz, 1H, H-4′), 7.69 (d, $J_{2''',3'''}$ = 8.8 Hz, 2H, H-2‴), 7.51 (t, $J_{5',4'} = J_{5',6'}$ = 8.0 Hz, 1H, H-5′), 7.46 (d, $J_{6',5'}$ = 8.0 Hz, 1H, H-6′), 6.55 (d, $J_{3''',2'''}$ = 8.8 Hz, 2H, H-3‴), 4.01 (d, $J_{2'',NHCO}$ = 5.3 Hz, 2H, H-2″), 3.57 (d, $J_{2,NHSOO}$ = 5.9 Hz, 2H, H-2), 2.72 (s, 3H, -C*H*$_3$); ^{13}C NMR (90.5 MHz, DMSO-d_6): δ 169.5 (C$_1$), 168.4 (C$_1$), 166.5 (-NH*C*O-), 152.0 (C$_{4'''}$), 141.1 (C$_{1'}$), 139.1 (C$_{3'}$), 129.0 (C$_{5'}$), 128.4 (C$_{2'''}$), 122.4 (C$_{4'}$), 120.6 (C$_{6'}$), 120.5 (C$_{1'''}$), 116.8 (C$_{2'}$), 110.2 (C$_{3'''}$), 43.6 (C$_2$), 43.2 (C$_{2''}$), 29.0 (-*C*H$_3$); IR (ATR) 3391, 3328, 2449, 1719, 1601, 1525, 1300, 1152 cm^{-1}. HRMS (ESI+): calcd. for [$C_{18}H_{20}N_4O_6S$+H]$^+$ [M+H]$^+$: 421.1182; found: 421.1182.

***N*-[(3-{[*N*-(Quinolin-3-ylcarbonyl)glycyl]amino}phenyl)sulfonyl]glycine, 17i.** Compound **17i** was prepared as described for **17c** by using compound **26i** (172 mg, 0.29 mmol), TFA (1.20 mL, 15.81 mmol) in CH_2Cl_2 (2 mL). The residue was solved in acetone and recrystalized adding CH_2Cl_2. The resulting white solid was washed with hexane to obtain **17i** (125 mg, 0.28 mmol, quant. yield). Mp = > 230 °C (from CH_2Cl_2). ^{1}H NMR (360 MHz, DMSO-d_6) δ 10.45 (s, 1H, –NH–1″), 9.37 (s, 1H, H-2‴), 9.32 (br t, $J_{NHCO,2''}$ = 5.5 Hz, 1H, -N*H*CO-), 8.97 (s, 1H, H-4‴), 8.17-8.11 (m, 3H, H-2′, H-5‴, H-8‴), 8.07 (m, 1H, -N*H*SO$_2$-), 7.92 (t, $J_{7''',6'''} = J_{7''',8'''}$ = 7.5 Hz, 1H, H-7‴), 7.83 (d, $J_{4',5'}$ = 7.7 Hz, 1H, H-4′), 7.74 (t, $J_{6''',5'''} = J_{6''',7'''}$ = 7.5 Hz, 1H, H-6‴), 7.55 - 7.47 (m, 2H, H-5′, H-6′), 4.19 (d, $J_{2'',NHCO}$ = 5.5 Hz, 2H, H-2″), 3.58 (d, $J_{2,NHSOO}$ = 5.8 Hz, 2H, H-2); ^{13}C NMR (90.5 MHz, DMSO-d_6): δ 170.2 (C$_1$), 168.1 (C$_{1''}$), 165.2 (-NH*C*O-), 148.6 (C$_{2'''}$), 147.7 (C$_{8a'''}$), 141.2 (C$_{1'}$), 139.4 (C$_{3'}$), 136.6 (C$_{4'''}$), 131.7 (C$_{7'''}$), 129.7 (C$_{5'}$), 129.3 (C$_{5'''}$), 128.2 (C$_{8'''}$), 127.7 (C$_{6'''}$), 126.7 (C$_{3'''}$), 126.6 (C$_{4a'''}$), 122.6 (C$_{4'}$), 121.1 (C$_{6'}$), 116.9 (C$_{2'}$), 43.8 (C$_{1''}$), 43.4 (C$_{1'}$); IR (ATR) 3253, 3083, 1648, 1594, 1518, 1428, 1314, 1155 cm^{-1}. HRMS (ESI+): calcd. for [$C_{20}H_{18}N_4O_6S$+H]$^+$ [M+H]$^+$: 443.1025; found: 443.1019.

3.2. Molecular modeling

The crystal structure of the AKAP79-derived peptide IAIIIT and CNA (PDB code 3LL8) was used for the docking calculations. For the docking, selected compounds were flexibly docked into the binding sites of receptor using AutoDock Vina. The Auto Dock Tools program was used to prepare the corresponding protein file. The protein was held rigid during the docking process, while ligands were allowed to be flexible. Docking simulations were performed using a grid box with dimensions of 25 × 25 × 30 Å, a search space of 10 binding modes, and the exhaustiveness parameter was set to 50.

3.3. Biological evaluation

3.3.1. Materials and methods

3.3.1.1. Cell lines. The mouse triple negative breast cancer 4T1 cell line was obtained from ATCC. Cells were cultured in DMEM high glucose with Glutamax supplemented with 10% fetal bovine serum (FBS), 100 U/ml penicillin and 100 μg/ml streptomycin, at 37 °C and 5% CO_2. Cells were expanded when reached 90% confluence. Viability was monitored before and after injection, that should be >90%. For cytotoxicity assays, HEK293T, CP15T, 768O, BxPC-3, PANC-1, HCI–H1650, A549 cell lines were grown in DMEM high glucose with Glutamax supplemented with 10% FBS and antibiotics.

Purified CD4$^+$ T cells were maintained in RPMI high glucose with Glutamax supplemented with 10% FBS, 100 U/ml penicillin and 100 μg/ml streptomycin, at 37 °C and 5% CO_2.

3.3.1.2. Fluorescence polarization. In fluorescence polarization (FP) competition assays of the CNA-SPRIEIT (NFATc2-derived peptide) interaction, 10 μM of human CNAα (amino acids 2–347) were pre-incubated with different concentrations of each inhibitory molecule in OptiPlate black 384-well flat-bottom plates (PerkinElmer Life Sciences) for 15 min at rt. Carboxyfluorescein (CF)- tagged NFATc2-derived SPRIEIT peptide (CF-SPRIEIT, 10 nM) was added to each well and incubated for 15 more min. Measurements were performed using a Victor™ X5 2030 Multilabel Reader (PerkinElmer Life Sciences) with excitation and emission wavelengths of 485 nm and 535 nm, respectively. All data were obtained from triplicates of at least three independent experiments.

3.3.1.3. Calcineurin phosphatase activity. CNA phosphatase activity towards the *p*-nitrophenylphosphate (pNPP) substrate was measured. Briefly, to determine the optimal concentration of CNA in the assay increasing concentrations of human CNAα (amino acids 2–347) were incubated with 5 mM pNPP in 100 μl final volume in 1x colorimetric assay buffer (20 mM Tris-HCl, 5 mM MgCl2, 1 mM EGTA, 0.02% β-mercaptoethanol and 0.1 mg/ml BSA) for 30 min at 30 °C in 96-well microtiter plates. Reaction was stopped by adding 10 μL 5 N NaOH and read 405 nm wavelength on a Victor™ X5 2030 Multilabel Reader (PerkinElmer Life Sciences).

For the assessment of CNA phosphatase activity inhibition by inhibitory hit molecules, preincubation of 0.5 μM human CNAα and inhibitors at 50 μM final concentration in 1x colorimetric assay buffer was carried out at 30 °C. After 30 min of incubation, pNPP was added to each well and incubated for 30 more min at 30 °C. Reaction was stopped and read as before. 50 μM $ZnCl_2$ was used as a negative control of CNA phosphatase activity. Background values obtained from a sample containing pNPP but not CNA was subtracted to each sample. Data were obtained from triplicates of three independent experiments.

3.3.1.4. NFATc activity. NFATc activity was determined by using a 3xNFAT-luc plasmid under the control of a NFATc promoter. Briefly, 7.5 × 10^4 HEK 293T cells per well were seeded in 48-well plates. The next day, each well was transfected with 100 ng of 3xNFAT-luc reporter plasmid and 1 ng pRLnull as internal control of transfection using $CaCl_2$ transfection technique. Then, 24 h after transfection, cells were treated with indicated concentration of the selected compounds for 2 h and then stimulated with 1 μM ionomycin (Io), 10 nM phorbol 12-myristate 13-acetate (PMA) and 10 mM $CaCl_2$, unless otherwise specified, for 4 h. Cyclosporin A (CsA, 1 μM) was used as positive control of CN phosphatase activity inhibition. After stimulation, cells were lysed, and crude extracts were analyzed for luciferase gene expression using the Dual-Luciferase Reporter Assay (Promega) following manufacturer's instructions on a Victor™ X5 2030 Multilabel Reader (PerkinElmer Life Sciences). Luciferase units were normalized to Renilla luciferase values.

The NFATc activity value, in the absence of any compound, was considered as 100% (positive control of CN activity). Data were obtained from at least three independent experiments. Data from Dose-Response experiment is plotted in a XY dispersion plot. IC_{50} values are calculated using non-linear regression curve (three-way) in GraphPad Prism8.

3.3.1.5. Human T cell proliferation and cytokine production. Human peripheral blood mononucleated cells (hPMBC) were isolated from healthy donors using Ficoll gradient. $CD4^+$ T cells were purified using autoMACS CD4 MicroBead human kit II (Miltenyi) according to manufacturer's instructions. $CD4^+$ T cells (1×10^5 cells/well) were seeded in 96-plate and treated with the indicated inhibitory compounds at 10 and 1 μM for 2 h. Next, the lymphocytes were activated with anti-CD3/anti-CD28 beads (Dynabeads human T-activator CD3/CD28, Gibco), at a ratio of 10 cells per bead. IL2 and IFNγ production was measured by ELISA (BD Pharmingen) in supernatants collected after 48 h of culture, following manufacturer's instructions. T cell proliferation was tested at 72 h by measuring [^{3}H]-thymidine incorporation on DNA. Briefly, 0.5 μCi of [^{3}H]- thymidine was added to each well after 48 h of culture. Twelve hours later, cells were harvested, and the incorporated radioactivity was measured using a scintillation counter (TopCount).

3.3.1.6. RNA extraction and real-time PCR. Isolated hPBMC were treated with each compound for 2 h. Cells were calcium stimulated with Ionomycin (1 μM), PMA (20 nM) and CaCl2 (10 mM) for 4 h. RNA from stimulated hPBMC was extracted using RNAeasy Kit (QIAGEN) following manufacturer's instructions. A total of 1 μg RNA were used to synthesize cDNA using Superscript III (Invitrogen). Quantitative PCR experiments were performed using probes from the Universal probe Library (UPL) (Roche). PCR reactions were carried out in triplicates in a Lightcycler 480 System (Roche). Human *HPRT1* gene amplification was used as housekeeping internal control. The sequences for the primers used are *hINFγ* fwd: GGCATTTTGAAGAATTGGAAAG, *hINFγ* rev: TTTGGATGCTCTGGTCATCTT, *hIL2* fwd: AAGTTTTACATGCCCAAGAAGG, *hIL2* rev: AAGTGAAAGTTTTTGCTTTGAGCTA, *hHPRT* fwd: TGACCTTGATTTATTTTGCATACC, *hHPRT* rev: CGGCAAGACGTTC AGTCCT.

3.3.1.7. Cell viability assay. The cytotoxicity of the NFATc inhibitory hit compounds in several human and mouse normal and tumor cell lines were determined by Cell Titer-Glo luminescent cell viability assay (Promega). Briefly, cells were treated with different concentrations (0, 1, 10 μM) of inhibitory compounds in a total volume of 100 μL/well for 2 h, and then 100 μL Cell Titer-Glo reagent was added into each well, and luminescence was recorded in a Victor X5 microplate reader (PerkinElmer). Cell viability was expressed as the mean percentage of luminescence values (RLU) of each sample relative to untreated control cells that were considered as 100%.

Animal experimentation is performed in accordance with local, national and European legislation. The *Parc Científic de Barcelona* (PCB) Ethical Committee approved all the procedures for Animal Experimentation and the procedure accepted by the competent authorities, Generalitat de Catalunya, is number 9912.

For primary tumor growth, 4T1 cells in exponential growth were injected (0.5×10^6 cells/animal) in 50 μl of a 1:1 mixture of DMEM and Matrigel (Corning, 356234) into the number four mammary fat pad mice (8 weeks, female, 18–19 g). A chip identified each animal and tumor growth was monitored biweekly measuring the diameter of tumors. When tumors reached a volume more than 100 mm^3 (at day 11 from cell injection), mice were distributed randomly in four groups of 9–10 animals each one. The treatment for each group was: 1) vehicle (DMSO), 2) compound **5a**, 3) compound **4** and 4) FK506, as a negative control of CN activity. Compounds **5a** and **4** were administered daily at 50 mg/kg/animal and FK506 at 5 mg/kg/animal (Monday to Friday). After 15 days of treatment animals were killed, tumors were surgically removed, and tissue samples were either immediately frozen or fixed in 4% paraformaldehyde and paraffin embedded.

3.3.1.8. Immunohistochemistry. For IHC analysis of mouse TNBC samples, paraffin sections (4 μm thickness) were blocked with 10% BSA for 1 h and then stained with anti-CD31 (rabbit-Abcam) by overnight incubation at 4 °C. Sections were washed and incubated with UltraVisionQuanto Detection System HRP (Thermo Scientific). Tissue sections were incubated with 3,3′-Diaminobenzidine (DAB) chromogen (Thermo Scientific) and counterstained with hematoxylin, dehydrated and mounted with DPX (Sigma). Antibody staining quantification was performed on at least five different high-power field (HPF) per sample, 20x magnification (Nikon Eclipse 80i).

Disclaimer

The authors declare no conflict of interest.

Authors contribution

The manuscript was written through contributions of all authors. All authors have given approval to the final version of the manuscript.

Declaration of competing interest

The authors declare that they have no known competing financial interest or personal relationships that could have appeared to influence the work reported in this paper.

Acknowledgments

The work was partially supported by funds from the Spanish Ministry of Economy, Industry, and Competitiveness (MINECO) (projects: SAF2015-66365, RTC-2015-3381-1, CTQ2016-75363-R and PID2019-106403RB-I00) co-financed with the European Fund for Regional Development (FEDER). We acknowledge additional support from Generalitat de Catalunya (2014-SGR-541 and 2017-SGR-191). We appreciate Juan José Lasarte's team in the analysis of cell proliferation and cytokine production analysis. A.B. was funded by the RTC-2015-3381-1 and SAF2015-66365 grants. ASM acknowledge the financial support from the Universitat Autònoma de Barcelona.

Appendix A. Supplementary data

Supplementary data to this article can be found online at https://doi.org/10.1016/j.ejmech.2022.114514.

References

[1] C.B. Klee, H. Ren, X. Wang, Regulation of the calmodulin-stimulated protein phosphatase, calcineurin, J. Biol. Chem. 273 (1998) 13367–13370, https://doi.org/10.1074/jbc.273.22.13367.
[2] J. Aramburu, A. Rao, C. Klee, Calcineurin: from structure to function, Curr. Top. Cell. Regul. (2000) 237–295.
[3] F. Macian, NFAT proteins: key regulators of T-cell development and function, Nat. Rev. Immunol. 5 (2005) 472–484, https://doi.org/10.1038/nri1632.
[4] M. Mancini, A. Toker, NFAT proteins: emerging roles in cancer progression, Nat. Rev. Cancer 9 (2009) 810–820, https://doi.org/10.1038/nrc2735.
[5] M.R. Muller, A. Rao, NFAT, immunity and cancer: a transcription factor comes of age, Nat. Rev. Immunol. 10 (2010) 645–656, https://doi.org/10.1038/nri2818.
[6] J. Roy, M.S. Cyert, Identifying new substrates and functions for an old enzyme: calcineurin, Cold Spring Harbor Perspect. Biol. 12 (2020), https://doi.org/10.1101/cshperspect.a035436 a035436.
[7] H. Li, P.G. Hogan, Calcineurin: a star is reborn, Cell Calcium 94 (2021), 102324, https://doi.org/10.1016/j.ceca.2020.102324.
[8] S.R. Sheftic, R. Page, W. Peti, Investigating the human calcineurin interaction network using the piLxVP SLiM, Sci. Rep. 6 (2016), 38920, https://doi.org/10.1038/srep38920.
[9] A. Rodríguez, J. Roy, S. Martínez-Martínez, M.D. López-Maderuelo, P. Niño-Moreno, L. Ortí, D. Pantoja-Uceda, A. Pineda-Lucena, M.S. Cyert, J.M. Redondo, A conserved docking surface on calcineurin mediates interaction with substrates

and immunosuppressants, Mol. Cell 33 (2009) 616–626, https://doi.org/10.1016/j.molcel.2009.01.030.
[10] H. Li, A. Rao, P. Hogan, Structural delineation of the calcineurin–NFAT interaction and its parallels to PP1 targeting interactions, J. Mol. Biol. 342 (2004) 1659–1674, https://doi.org/10.1016/j.jmb.2004.07.068.
[11] H. Li, L. Zhang, A. Rao, S. Harrison, P. Hogan, Structure of calcineurin in complex with PVIVIT peptide: portrait of a low-affinity signalling interaction, J. Mol. Biol. 369 (2007) 1296–1306, https://doi.org/10.1016/j.jmb.2007.04.032.
[12] S. Grigoriu, R. Bond, P. Cossio, J. Chen, N. Ly, G. Hummer, R. Page, M. Cyert, W. Peti, The molecular mechanism of substrate engagement and immunosuppressant inhibition of calcineurin, PLoS Biol. 11 (2013), e1001492, https://doi.org/10.1371/journal.pbio.1001492.
[13] J. Roy, M. Cyert, Cracking the phosphatase code: docking interactions determine substrate specificity, Sci. Signal. 2 (2009) re9, https://doi.org/10.1126/scisignal.2100re9.
[14] C. Wigington, J. Roy, N. Damle, V. Yadav, C. Blikstad, E. Resch, C. Wong, D. Mackay, J. Wang, I. Krystkowiak, D. Bradburn, E. Tsekitsidou, S. Hong, M. Kaderali, S. Xu, T. Stearns, A. Gingras, K. Ullman, Y. Ivarsson, N- Davey, M. Cyert, Systematic discovery of short linear motifs decodes calcineurin phosphatase signaling, Mol. Cell. 79 (2020) 342–358, https://doi.org/10.1016/j.molcel.2020.06.029, e12.
[15] H. Li, M.D. Pink, J.G. Murphy, A. Stein, M.L. Dell'Acqua, P.G. Hogan, Balanced interactions of calcineurin with AKAP79 regulate Ca2+-calcineurin-NFAT signaling, Nat. Struct. Mol. Biol. 19 (2012) 337–345, https://doi.org/10.1038/nsmb.2238.
[16] Y. Li, S.R. Sheftic, S. Grigoriu, C.D. Schwieters, R. Page, W. Peti, The structure of the RCAN1:CN complex explains the inhibition of and substrate recruitment by calcineurin, Sci. Adv. 6 (2020), eaba3681, https://doi.org/10.1126/sciadv.aba3681.
[17] S. Martínez-Martínez, L. Genescà, A. Rodríguez, A. Raya, E. Salichs, F. Were, M. López-Maderuelo, J. Redondo, S. de la Luna, The RCAN carboxyl end mediates calcineurin docking-dependent inhibition via a site that dictates binding to substrates and regulators, Proc. Natl. Acad. Sci. Unit. States Am. 106 (2009) 6117–6122, https://doi.org/10.1073/pnas.0812544106.
[18] M.C. Mulero, A. Aubareda, M. Orzaez, J. Messeguer, E. Serrano-Candelas, S. Martinez-Hoyer, A. Messeguer, E. Perez-Paya, M. Perez-Riba, Inhibiting the calcineurin-NFAT (nuclear factor of activated T cells) signaling pathway with a regulator of calcineurin-derived peptide without affecting general calcineurin phosphatase activity, J. Biol. Chem. 284 (2009) 9394–9401, https://doi.org/10.1074/jbc.M805889200.
[19] C. Kissinger, H. Parge, D. Knighton, C. Lewis, L. Pelletier, A. Tempczyk, V. Kalish, K. Tucker, R. Showalter, E. Moomaw, L. Gastinel, N. Habuka, X. Chen, F. Maldonado, J. Barker, R. Bacquet, J. Villafranca, Crystal structures of human calcineurin and the human FKBP12–FK506–calcineurin complex, Nature 378 (1995) 641–644.
[20] J.P. Griffith Kim, E.E. Kim, M.D. Sintchak, J.A. Thomson, M.J. Fitzgibbon, M. A. Fleming, P.R. Caron, K. Hsiao, M.A. Navia, X-ray structure of calcineurin inhibited by the immunophilin-immunosuppressant FKBP12-FK506 complex, Cell 82 (1995) 507–522, https://doi.org/10.1016/0092-8674(95)90439-5.
[21] L. Jin, S. Harrison, Crystal structure of human calcineurin complexed with cyclosporin A and human cyclophilin, Proc. Natl. Acad. Sci. Unit. States Am. 99 (2002) 13522–13526, https://doi.org/10.1073/pnas.212504399.
[22] Q. Huai, H. Kim, Y. Liu, Y. Zhao, A. Mondragon, J. Liu, H. Ke, Crystal structure of calcineurin-cyclophilin-cyclosporin shows common but distinct recognition of immunophilin-drug complexes, Proc. Natl. Acad. Sci. Unit. States Am. 99 (2002) 12037–12042, https://doi.org/10.1073/pnas.192206699.
[23] M.J. Mihatsch, M. Kyo, K. Morozumi, Y. Yamaguchi, V. Nickeleit, B. Ryffel, The side-effects of ciclosporine-A and tacrolimus, Clin. Nephrol. 49 (1998) 356–363. PMID: 9696431.
[24] S. Martinez-Martinez, J. Redondo, Inhibitors of the calcineurin/NFAT pathway, Curr. Med. Chem. 11 (2004) 997–1007, https://doi.org/10.2174/0929867043455576.
[25] M.T. Matsoukas, A. Aranguren-Ibanez, T. Lozano, V. Nunes, J.J. Lasarte, L. Pardo, M. Perez-Riba, Identification of small-molecule inhibitors of calcineurin-NFATc signaling that mimic the PxIxIT motif of calcineurin binding partners, Sci. Signal. 8 (2015) ra63, https://doi.org/10.1126/scisignal.2005918.
[26] For a review, see: C. Hansch, P.G. Sammes, J.B. Taylor, Comprehensive Medicinal Chemistry, vol. 2, Pergamon Press, Oxford, 1990 (Chapter 7).1.
[27] M. Izquierdo-Serra, M. Gascón-Moya, J.J. Hirtz, S. Pittolo, K.E. Poskanzer, E. Ferrer, R. Alibés, F. Busqué, R. Yuste, J. Hernando, P. Gorostiza, Two-photon neuronal and astrocytic stimulation with azobenzene-based photoswitches, J. Am. Chem. Soc. 136 (2014) 8693–8701, https://doi.org/10.1021/ja5026326.
[28] R. Solórzano, O. Tort, J. García-Pardo, T. Escribà, J. Lorenzo, M. Arnedo, D. Ruiz-Molina, R. Alibés, F. Busqué, F. Novio, Versatile iron-catechol based nanoscale coordination polymers antiretroviral ligand functionalization and their use as efficient carriers in HIV/AIDS therapy, Biomater. Sci. 7 (2019) 178–186, https://doi.org/10.1039/C8BM01221K.
[29] G. Cabré, A. Garrido-Charles, A. González Lafont, W. Moormann, D. Langbehn, D. Egea, J.-M. Lluch, R. Herges, R. Alibes, F. Busque P, J. Gorostiza, Hernando, Synthetic photoswitchable neurotransmitters based on bridged azobenzenes, Org. Lett. 21 (2019) 3780–3784, https://doi.org/10.1021/acs.orglett.9b01222.
[30] M. Gascón-Moya, A. Pejoan, M. Izquierdo-Serra, S. Pittolo, G. Cabré, J. Hernando, R. Alibés, P. Gorostiza, F. Busqué, An optimized glutamate receptor photoswitch with sensitized azobenzene isomerization, J. Org. Chem. 80 (2015) 9915–9925, https://doi.org/10.1021/acs.joc.5b01402.
[31] C.T. Quang, S. Leboucher, D. Passaro, L. Fuhrmann, M. Nourieh, A. Vincent-Salomon, J. Ghysdael, The calcineurin/NFAT pathway is activated in diagnostic breast cancer cases and is essential to survival and metastasis of mammary cancer cells,, Cell Death Dis. 6 (2015), https://doi.org/10.1038/cddis.2015.14 e1658.
[32] S. Jauliac, C. Lopez-Rodriguez, L.M. Shaw, L.F. Brown, A. Rao, A. Toker, The role of NFAT transcription factors in integrin-mediated carcinoma invasion, Nat. Cell Biol. 4 (2002) 540–544, https://doi.org/10.1038/ncb816.
[33] S. Martínez-Hoyer, S. Solé-Sánchez, F. Aguado, S. Martínez-Martínez, E. Serrano-Candelas, J.L. Hernández, M. Iglesias, J.M. Redondo, O. Casanovas, R. Messeguer, M. Pérez-Riba, A novel role for an RCAN3-derived peptide as a tumor suppressor in breast cancer, Carcinogenesis 36 (2015) 792–799, https://doi.org/10.1093/carcin/bgv056.
[34] J.-J. Qin, S. Nag, W. Wang, J. Zhou, W.-D. Zhang, H. Wang, R. Zhang, NFAT as cancer target: mission possible? Biochim. Biophys. Acta 1846 (2014) 297–311, https://doi.org/10.1016/j.bbcan.2014.07.009.
[35] A. Spreafico, J. Tentler, T. Pitts, A. Tan, M. Gregory, J. Arcaroli, P. Klauck, M. McManus, R. Hansen, J. Kim, L. Micel, H. Selby, T. Newton, K. McPhillips, D. Gustafson, J. DeGregori, W. Messersmith, R. Winn, S. Eckhardt, Rational combination of a MEK inhibitor, selumetinib, and the wnt/calcium pathway modulator, cyclosporin A, in preclinical models of colorectal cancer, Clin. Cancer Res. 19 (2013) 4149–4162, https://doi.org/10.1158/1078-0432.CCR-12-3140.
[36] J. Aramburu, M.B. Yaffe, C. López-Rodríguez, L.C. Cantley, P.G. Hogan, A. Rao, Affinity-driven peptide selection of an NFAT inhibitor more selective than cyclosporin A, Science 285 (5436) (1999) 2129–2133, https://doi.org/10.1126/science.285.5436.2129.
[37] G. Crabtree, E. Olson, NFAT signaling: choreographing the social lives of cells, Cell 109 (2002) S67–S79, https://doi.org/10.1016/s0092-8674(02)00699-2.
[38] M. Pan, Y. Xiong, F. Chen, NFAT gene family in inflammation and cancer, Curr. Mol. Med. 13 (2013) 543–554, https://doi.org/10.2174/1566524011313040007.
[39] U. Testa, G. Castelli, E. Pelosi, Breast cancer: a molecularly heterogenous disease needing subtype-specific treatments, Med. Sci. 8 (2020) 18, https://doi.org/10.3390/medsci8010018.
[40] R. Mohammed, I. Ellis, A. Mahmmod, E. Hawkes, A. Green, E. Rakha, S. Martin, Lymphatic and blood vessels in basal and triple-negative breast cancers: characteristics and prognostic significance, Mod. Pathol. 24 (2011) 774–785, https://doi.org/10.1038/modpathol.2011.4.
[41] B. Linderholm, H. Hellborg, U. Johansson, G. Elmberger, L. Skoog, J. Lehtiö, R. Lewensohn, Significantly higher levels of vascular endothelial growth factor (VEGF) and shorter survival times for patients with primary operable triple-negative breast cancer, Ann. Oncol. 20 (2009) 1639–1646, https://doi.org/10.1093/annonc/mdp062.
[42] S. Siamakpour-Reihani, J. Caster, D. Bandhu Nepal, A. Courtwright, E. Hilliard, J. Usary, D. Ketelsen, D. Darr, X. Shen, C. Patterson, N. Klauber-DeMore, The role of calcineurin/NFAT in SFRP2 induced angiogenesis—a rationale for breast cancer treatment with the calcineurin inhibitor tacrolimus, PLoS One 6 (2011), e20412, https://doi.org/10.1371/journal.pone.0020412.
[43] G. Hernández, O. Volpert, M. Íñiguez, E. Lorenzo, S. Martínez-Martínez, R. Grau, M. Fresno, J. Redondo, Selective inhibition of vascular endothelial growth factor–mediated angiogenesis by cyclosporin a: roles of the nuclear factor of activated T cells and cyclooxygenase 2, J. Exp. Med. 193 (2001) 607–620, https://doi.org/10.1084/jem.193.5.607.
[44] A. Kaunisto, W. Henry, L. Montaser-Kouhsari, S. Jaminet, E. Oh, L. Zhao, H. Luo, A. Beck, A. Toker, NFAT1 promotes intratumoral neutrophil infiltration by regulating IL8 expression in breast cancer, Mol. Oncol. 9 (2015) 1140–1154, https://doi.org/10.1016/j.molonc.2015.02.004.
[45] A. Baeza, Tumor targeted nanocarriers for immunotherapy, Molecules 25 (2020) 1508, https://doi.org/10.3390/molecules25071508.
[46] Y. Yao, Y. Zhou, L. Liu, Y. Xu, Q. Chen, Y. Wang, S. Wu, Y. Deng, J. Zhang, A. Shao, Nanoparticle-based drug delivery in cancer therapy and its role in overcoming drug resistance, Front. Mol. Biosci. 7 (2020) 193, https://doi.org/10.3389/fmolb.2020.00193.